



3 1176 00162 8529

NASA TM-81885

NASA Technical Memorandum 81885

NASA-TM-81885 19800023853

FLIGHT PERFORMANCE OF THE TCV B-737
AIRPLANE AT MONTREAL/DORVAL INTERNATIONAL
AIRPORT, MONTREAL, CANADA, USING
TRSB/MLS GUIDANCE

William F. White and Leonard V. Clark

FOR REFERENCE

NOT TO BE TAKEN FROM THE ROOM

SEPTEMBER 1980

LIBRARY COPY

OCT 1 1980

LANGLEY RESEARCH CENTER
LIBRARY, NASA
HAMPTON, VIRGINIA



National Aeronautics and
Space Administration

Langley Research Center
Hampton, Virginia 23665

SUMMARY

On April 3-16, 1978, the Terminal Configured Vehicle (TCV) B-737 airplane was flown at Montreal/Dorval International Airport in Montreal, Canada, in support of the Federal Aviation Administration (FAA) demonstration of the U.S. candidate Time Reference Scanning Beam (TRSB) Microwave Landing System (MLS).

The objective of the National Aeronautics and Space Administration (NASA) participation in the TRSB/MLS demonstration program was to demonstrate practical utilization of MLS guidance for curved, noise-abatement approaches and at the same time acquire useful pilot operational experience. The formal demonstration flights at Dorval consisted of 59 automatic approaches. The demonstration flights were preceded by other manual and automatic checkout flights to verify the acceptability of the processed MLS parameters, and to evaluate the performance of the airplane along several candidate curved-path approaches. On the basis of results from these checkout flights two approaches were selected for demonstration. The report presents a summary of the flight performance of the TCV airplane during the demonstration automatic approaches and landings while utilizing TRSB/MLS guidance. Detailed analyses of the performance data are not presented herein.

INTRODUCTION

The NASA Langley Research Center's Terminal Configured Vehicle (TCV) program operates a highly modified Boeing 737 airplane which contains a second research cockpit in addition to a large amount of experimental navigation, guidance, and control equipment for conducting flight research on advanced avionics systems and displays. The FAA requested that NASA use the TCV B-737 to provide demonstrations of the TRSB/MLS being proposed by the United States as a new international standard landing guidance system to replace the presently used Instrument Landing System (ILS) and Precision Approach Radar (PAR). The first such demonstration was conducted at the FAA's National Aviation Facilities Experimental Center (NAFEC) at Atlantic City, New Jersey in May 1976 for members of the International Civil Aviation Organization (ICAO), industry and government officials, and representatives of the news media. The flight results from the NAFEC demonstration are documented in references 1 and 2 which also include descriptions of the TCV airplane equipment, MLS processing, and control laws. The latter were modifications of the original ILS control laws, since insufficient time was available to develop new control laws designed for MLS. Similar demonstrations were subsequently requested for Buenos Aires, Argentina, in October 1977, for New York in December 1977, and for Montreal, Canada, in April 1978.

N80-32361 #

This report summarizes the flight performance results of the TCV airplane during the demonstration automatic approaches and landings conducted at the Montreal/Dorval International Airport. The TRSB system demonstrated at Dorval was installed on runway 28 and consisted of the Basic Wide azimuth and elevation subsystems and a precision L-band DME. Observers carried on these demonstration flights were primarily attendees of a meeting of the All-Weather Operations Division of ICAO. For comparison purposes references 3 and 4 describe the previous flight performance of the TCV B-737 while utilizing TRSB/MLS guidance at Jorge Newbery Airport (Buenos Aires) and John F. Kennedy Airport (New York).

ABBREVIATIONS AND SYMBOLS

AZ	Microwave Landing System azimuth guidance
CAT I	Category I Landing Minima 71m (200 ft) decision height, 732m (2400 ft) runway visual range
CAT II	Category II Landing Minima 30.5m (100 ft) decision height, 366m (1200 ft) runway visual range
CRT	Cathode Ray Tube
DELTH	Vertical error signal input to autoland control law
DELTY	Lateral error signal input to autoland control law (negative of cross track error)
DH	Decision Height
DME	Distance Measurement Equipment
EADI	Electronic Attitude Director Indicator
EHSI	Electronic Horizontal Situation Indicator
EL	Microwave Landing System elevation guidance
FAA	Federal Aviation Administration
FAF	Final Approach Fix
GPIP	Glide Path Intercept Point
\dot{h}_{MLS}	Vertical speed derived from Microwave Landing System
HER	Vertical error signal input to RNAV control law (negative of altitude error)
ICAO	International Civil Aviation Organization

IDD	Inertial and Dual DME area navigation mode
IDX	Inertial and Single DME area navigation mode
ILS	Instrument Landing System
INS	Inertial Navigation System
IXX	Inertial area navigation mode
MLS	Microwave Landing System
MSL	Mean Sea Level
NAFEC	National Aviation Facilities Experimental Center
NASA	National Aeronautics and Space Administration
NCDU	Navigation Control and Display Unit
PAR	Precision Approach Radar
PCM	Pulse Code Modulation
PDME	Precision Distance Measurement Equipment
RNAV	Area navigation
R_{Rhumb}	Rhumb line distance from GPIIP ($60 \times \Delta \text{latitude} \div \cosine \text{ of the course angle from true North}$)
SID	Standard Instrument Departure
STAR	Standard Terminal Arrival Route
TCV	Terminal Configured Vehicle
TRSB	Time Reference Scanning Beam
TV	Television
VOR	Very high frequency Omnidirectional Range
\hat{X}	Estimated distance along runway centerline extended from MLS azimuth antenna
XTK	Lateral error signal input to RNAV control law
\hat{Y}	Estimated perpendicular distance from runway centerline extended
Δh	Height above Glide Path Intercept Point

ΔH	Vertical distance from glide path
ΔHER	Change in HER at conventional-to-MLS RNAV transition
ΔXTK	Change in XTK at conventional-to-MLS RNAV transition
Δy	Perpendicular distance from runway centerline
τ	Flare time constant

TCV RESEARCH AIRPLANE

The TCV Program operates a Boeing 737-100 airplane (figure 1) to conduct flight research aspects of the program. The airplane is equipped with a special research flight deck, located about 6m (20 ft) aft of the standard flight deck. An extensive array of electronic equipment and data recording systems is installed throughout the former passenger cabin (figure 2).

The airplane can be flown from the aft flight deck using advanced electronic displays and semi-automatic or automatic control systems that can be programmed for research purposes. Two safety pilots located in the front flight deck are responsible for all phases of flight safety and most traffic clearances. Two research pilots usually fly the airplane from the aft cockpit during test periods, which can last from take-off through landing. The only normal flight systems that cannot be controlled from the aft flight deck are the landing gear and the speed brakes, which are operated by the safety pilots in response to annunciators. The safety pilots can take control of the airplane at any time by overpowering the aft flight deck controls or by disengaging the aft flight deck.

The aft flight deck (figure 3) includes three monochromatic Cathode Ray Tube (CRT) displays that are available to each research pilot. The lower display is the Navigation Control and Display Unit (NCDU) which allows each pilot to control and monitor the airplane's navigation computer. The computer can access airway, Standard Instrument Departure (SID), Standard Terminal Arrival Route (STAR), and runway data for the geographic area of interest.

The center display is an Electronic Horizontal Situation Indicator (EHSI) that provides each pilot with a pictorial navigation display of the airplane's position relative to desired guidance path, flight plan waypoints, and selectable local points of interest such as airfields, obstructions and radio navigation aids.

The top display is an Electronic Attitude Director Indicator (EADI) that provides the pilots with a display of the airplane's pitch and roll attitude for instrument flight. Other symbols for flight path acceleration, flight path angle (actual and commanded), lateral and vertical guidance, and speed error are integrated into the EADI display format. A forward-looking television image (from a TV camera located in the airplane's nose) can be presented on the EADI in registration with the symbols. A computer-generated runway drawing, showing the true

perspective of the runway (based on navigation position estimates) can also be displayed during approach and landing.

The TCV airplane's navigation, autoland and autothrottle systems permit the plane to fly complex two-, three-, and four-dimensional (position and time control) flight paths. The flight plan can either be programmed before takeoff or developed and modified in flight through the navigation computer's keyboard. An on-board data acquisition system records pertinent flight information for analysis after a test. Information can also be transmitted to a ground station within a range of 50 n. mi.

MLS APPROACHES INTO MONTREAL/DORVAL INTERNATIONAL AIRPORT

The flight paths used at Montreal/Dorval International Airport are shown in figure 4 superposed on a map of the area. The two approach paths (STARs) chosen for the test/demonstration, DORA2 and DORA5, are shown in detail in figures 5 and 6 and described below.

STAR DORA2. After takeoff the published noise abatement procedure was followed. This called for maximum climb to 3000 ft MSL on runway heading. A normal climb was then continued to 5000 ft MSL, with a left turn to follow the Trans-Canada Highway. After reaching 5000 ft, which assured safe clearance from traffic following the SID at 4000 ft, a turn to the southeast was made to enter the STAR at the initial waypoint just south of the town of Chateaugay. A 4.1° glide path was intercepted at the beginning of the turn to base leg, about 8 n. mi. southeast of the airport. The steep descent was maintained until past the industrial and commercial area indicated by the large black buildings on the map. Once over the railroad yard, a gradual turn was started to intercept the final approach course 1.1 n. mi. from threshold. Transition to a 3° glide path was made at the start of the turn to final approach.

STAR DORA5. Departure procedures were the same as for DORA2, except that after reaching 5000 ft a turn was made to follow the St. Lawrence River on the downwind leg. Upon reaching the published procedure turn area for the ILS Localizer Back Course approach to runway 28, a descending turn was made to intercept the extended runway centerline about 7 n. mi. from threshold at an altitude of about 300 ft above the procedure turn altitude. However, rather than fly straight in and descend to 1500 ft over a residential area of Montreal, the turn was continued to keep the flight path above a commercial and industrial area paralleling a canal, railroad tracks, and a major expressway. A right turn was then made to follow the approximate track of DORA2. For this STAR, the use of shorter turn radii resulted in interception of final approach at a distance of 1.4 n. mi.

The control law schedule of the TCV B-737 during the DORA2 automatic approaches is depicted in figure 7. The control law schedule for the DORA5 approaches was similar.

MLS EQUIPMENT AND PROCESSING

The MLS ground system at the Montreal/Dorval International Airport was comprised of the basic wide AZ subsystem with $\pm 60^\circ$ coverage, the basic wide EL subsystem, and a Precision DME co-located with the AZ antenna. The equipment installation is illustrated in figure 8. Due to equipment failures, the PDME was out of service for several days at the beginning of the demonstration period. As an emergency measure, the airborne software was modified to allow use of the ILS DME on runway 6L. After test flights and suitable adjustment of constants to correct for the bias errors, the first three demonstration flights (8 approaches and landings) were successfully conducted using the substitute DME.

In order to accommodate side-by-side operation with the British Doppler MLS, the AZ antenna was offset from the runway centerline by 5.6m. This was corrected for by making the usual conversion from conical to rectangular coordinates, using the AZ antenna as the origin, then computing the cross track error for the autoland system as

$$\text{DELTY} = -\hat{Y} + 5.6\text{m}$$

Through an oversight this correction was not included in the computation of latitude and longitude, so that the navigation computer always had an error of 5.6m perpendicular to the runway centerline.

FLIGHT RESULTS AND DISCUSSION

Flight performance data obtained during the TRSB/MLS demonstration flights of the TCV B-737 at Montreal/Dorval International Airport are presented in table I. These data are presented in chronological order for selected points along the approach and landing path: At conventional-to-MLS RNAV transition, the final approach fix, the CAT I decision height, the CAT II decision height, flare initiation, and touchdown. The final approach fix data are shown as determined from both the navigation and flight control computers. At this point the lateral axis was generally still being controlled by the RNAV system and the longitudinal axis was in the autoland glide path tracking mode. The data therefore represent flight technical error of the RNAV system in the lateral axis, and of the autoland system in the longitudinal axis. Twenty-four DORA2 approaches and thirty-five DORA5 approaches were flown. Fifty-eight of these approaches resulted in automatic landings. The mean values and estimated standard deviations of the flight performance data are shown at the bottom of the table.

Data are missing from the table due to a combination of circumstances. Since a new experimental flare control law was being used for these flights, the flight control computer flight technical errors DELTY and DELTH were replaced on many runs by variables which would allow analysis of the flare law performance. Ordinarily these variables could also be retrieved from autopilot formatter data, but the formatters malfunctioned on a number of flights and the data were lost.

The winds presented in table I at the time of flare were derived from the onboard navigation computer. The conventional presentation format is followed; the first pair of numbers is the true direction from which the wind is blowing expressed to the nearest 10-degree increment (e.g. 27 = 270 degrees) and the second pair is the wind speed expressed in knots.

Typical Approach Data

Representative data for each of the approaches are presented in figures 9 and 10 showing the cross track and altitude deviations from the planned curved approach path according to the processed MLS signals. These data do not indicate performance of the MLS, but rather performance of the airplane's guidance system utilizing MLS. However, analysis of photo-theodolite tracking data from reference 1 indicates that the MLS guidance accuracy is comparable to the photo-theodolite tracker accuracy, and therefore the MLS-derived position errors may be considered a good indication of path following error magnitudes. This is substantiated by a comparison of data from references 4 and 5. It should be noted, however, that these data were all obtained at elevation angles of the order of 3 to 4 degrees. During the Montreal flights, substantial altitude disagreements were noted between barometric and MLS-derived values, especially on the DORA5 path where initial elevation angles upon entry to MLS coverage were nearer 10 degrees. These differences were significant enough that the pilots modified their procedures and did not switch to MLS guidance while the VERT PATH mode of the autopilot was engaged, in order to avoid pitch attitude transients caused by the step change in indicated vertical error.

The plots in figures 9 and 10 are annotated to indicate various discrete events along the approach paths according to the control law schedule shown in figure 7. At TRSB ENABLE the airplane guidance changes from conventional 2D-RNAV (IDD/IDX/IXX modes) to MLS RNAV. After observing the altitude error and making corrections if necessary the 3D-RNAV mode was engaged. During the constant 3-degree curved descent phase the airplane approaches the final 3-degree planar glide path from above. The switch from RNAV to autoland vertical guidance occurs when the airplane comes within 0.108 degrees of the planar glide path. A discontinuity in altitude error may be noted on figures 9 and 10 at this point due to the differences in altitude between the curved and planar glide paths. The switch from RNAV to autoland guidance in the lateral axis occurs near the final approach fix, when the aircraft rolls out to less than a 3-degree bank angle, with a ground track angle within 0.27 degrees of runway heading and an azimuth angle error of not more than 0.2 degrees from runway centerline. Decrab occurs at an altitude of 45.7m (150 ft) above the ground provided that lateral guidance is in the autoland mode. Flare initiation occurs at an altitude of 42 ft above ground.

The variables XTK and the negative of HER represent flight technical error for the lateral and longitudinal axes of the autopilot when in the RNAV control mode, respectively. In the autoland control mode, the

corresponding errors are DELTY and DELTH. As previously discussed, these variables were not available for a number of runs during these demonstration flights.

Conventional-To-MLS RNAV Transition Offsets

Figures 11 and 12 present a summary of the TRSB-derived position estimates of X and Y at the time of the TCV B-737 airplane transition from conventional RNAV guidance. The location of this transition point was dependent upon first receiving valid MLS azimuth, elevation and precision range data for more than 10 seconds, and a subsequent pilot-initiated switchover at his discretion after receiving an MLS valid annunciation. The DORA5 path provided considerably more time within MLS coverage than the DORA2 path. However, during the downwind portions of this path the aircraft heading is such that the AZ antenna is nearly directly behind the aircraft, where antenna coverage is poor from the single front-mounted antenna. Even so, the data show reception was good enough that many of the transitions to MLS guidance occurred during this phase of flight.

Figure 13 summarizes conventional-to-MLS RNAV transition data for the approaches shown in figures 11 and 12. The numbers represent the change in XTK and HER (flight technical error) upon switching to MLS guidance. The mean values of $\Delta XTK = -95.3m$ and $-\Delta HER = -52.8m$ indicate that the aircraft was typically to the left of the intended horizontal track, and below the intended vertical path. A significant difference in the offsets was noted for the two STARs, however. For the DORA2 path the mean values were $\Delta XTK = -26.3m$ and $-\Delta HER = -39.0m$. For the DORA5 path the corresponding numbers were $-142.6m$ and $-62.3m$. The largest horizontal path offset observed was $273.1m$, and the largest altitude offset was $-118.3m$.

Automatic Approaches and Landings

Figure 14 schematically depicts the FAA certification criteria for approaches and automatic landings using ILS guidance, taken from references 6, 7, and 8. Some additional points used for data analysis are also shown. The flight performance data from table I are compared with the certification criteria in figures 15 through 19 and figure 21 in order to provide some quantitative aspects of the TCV B-737 approach and landing performance utilizing MLS guidance in lieu of conventional ILS guidance.

Final Approach Fix Delivery Errors. Figures 15 and 16 present the autopilot guidance errors at the final approach fix as determined from the navigation and flight control computers, respectively. At this point the cross track flight technical error is represented by XTK (figure 15), since localizer mode engage has either not yet occurred, or has only just occurred such that the aircraft has not yet had time to react to a change in control laws. The vertical flight technical error is given by ΔH (figure 16), since the glide path tracking mode of the autoland system was engaged earlier during the turn to final.

Several points require discussion with regard to discrepancies between figures 15 and 16. In figure 15 it can be seen that the RNAV system performance differed for the two approach paths. The mean value of XTK for the DORA5 path was 15m to the right of the mean for DORA2. This can be attributed to the steeper bank angles used on DORA5 and to the additional maneuvering just prior to turning final on that path. In order to cancel some of the RNAV overshoot error, the FAF waypoint was moved slightly to the left of runway centerline for DORA5. The effect is seen in figure 16, where the actual MLS-derived aircraft position error differed by only 7.1m at the FAF for DORA2 vs. DORA5. It is also apparent from a comparison of cross-track error discontinuity at localizer mode engage in figures 9 and 10.

A second comment involves the previously-mentioned failure to account for the AZ antenna offset in the RNAV computations. Figure 16 indicates that for the DORA2 path, the mean delivery error at the FAF was only 0.8m whereas the RNAV system guidance error mean was -6.7m at that point. Most of that discrepancy (5.6m) is due to the AZ antenna offset from centerline.

A final point concerns the difference of 1.9m in altitude error between figures 15 and 16. The aircraft actually tracks a computed glide path rather than flying the 3° EL beam. All MLS position measurements are translated to the aircraft center of gravity, and the computed glide path may be adjusted so that flare initiation occurs at a known main wheel height above the runway. In this case the GPIIP calculated for the autoland system was inadvertently set to be 44.8m different from the RNAV path GPIIP, which resulted in the RNAV glide path being 2.3m below the path being tracked by the autoland system.

Localizer and Glide Path Tracking Errors. Figures 17 through 19 show the MLS-derived position errors at the CAT I decision height, the CAT II decision height, and at flare initiation, respectively. Figure 17 includes a point indicating that the aircraft was more than 5m below glide path. An analysis of this run is shown in figure 20, where it can be seen that the large error is due to a combination of a windshear a few seconds before completing the turn to final approach, and a late and unfortunately timed reconfiguration and speed change for landing. A 20 knot speed reduction and flap change from 25 to 40° was initiated at an altitude above the runway of about 400 ft while the aircraft was still recovering from the effects of the shear. A high sink rate developed and the recovery was delayed somewhat by the fact that actual glide path deviation exceeded the limits of DELTH fed to the glide path tracking control law. The autoland system was therefore reacting to an error signal which indicated a large but decreasing error, whereas the actual error was larger yet and still increasing.

As shown in figure 18, the TCV B-737 performance was considerably better than that required for Categories II and IIIa autopilot certification, as given in references 6 and 7.

Touchdown Performance Touchdown time determination was made using an expanded scale time history plot of vertical acceleration and both main outboard wheel speeds. The time of touchdown was fixed as being the time at which a positive increase was seen on any one of these three variables and validated by the subsequent behavior of the other two. This data was sampled by the aircraft data acquisition system at a 40 Hz rate.

Touchdown position was determined from MLS-derived estimates of latitude and longitude, from which a rhumb-line calculation was made of distance from the GPIP. This gave very nearly the same results as the use of the position estimate X, but the latter was not used due to its unavailability on a number of runs where the autopilot data formatter malfunctioned.

Touchdown sink rate was determined from the MLS-derived vertical speed. The mean value of touchdown sink rate for all of the TCV B-737 landings was -0.89 m/s with a 2σ dispersion of ± 0.38 m/s.

Figure 21 presents a summary of the touchdown performance data for the TCV B-737 automatic landings. These data are compared with the FAA criteria for autoland systems (reference 8). In the figure the longitudinal location of the specified touchdown footprint is arbitrarily located with respect to the GPIP. Figure 21 does not include all of the touchdown data since the lateral error was not available for some of the runs. The longitudinal dispersion shown in the figure therefore differs slightly with the value in table I, which includes all of the landings. For all landings, the mean touchdown point was 80.1m past the GPIP with a dispersion of 93m, 2σ . This represents a large reduction in dispersion over that experienced in previous MLS demonstrations (references 2-4) due to the use of the new variable τ flare control law. The mean value of wind speed at flare initiation was 15 knots. The mean wind direction was 270 degrees, almost a direct headwind for landings on runway 28 (true runway heading of 267.7°).

CONCLUDING REMARKS

The NASA TCV B-737 participation in the TRSB-MLS demonstration at Montreal, Canada, was completed just prior to the conclusion of the ICAO All Weather Operations Division meeting which voted to adopt TRSB-MLS as the new international landing guidance system. The successful approaches and landings at Montreal/Dorval International Airport that were flown by the TCV B-737 proved the capability of MLS for providing adequate guidance for automatically flying curved, noise-abatement type approaches and landings with short finals.

REFERENCES

1. Paulson, C. V. and Weener, E. F.: The TCV B-737 Flight Performance During the Demonstration of the Time Reference Scanning Beam Microwave Landing System to the International Civil Aviation Organization All Weather Operations Panel. Boeing Commercial Airplane Company Document No. D6-44291, February 1977.
2. White, William F., et al.: Flight Demonstrations of Curved, Descending Approaches and Automatic Landings Using Time Reference Scanning Beam Guidance. NASA Technical Memorandum 78745, May 1978.
3. White, William F. and Clark, Leonard V.: Flight Performance of the TCV B-737 Airplane at Kennedy Airport Using TRSB/MLS Guidance. NASA Technical Memorandum 80148, July 1979.
4. White, William F. and Clark, Leonard V.: Flight Performance of the TCV B-737 Airplane at Jorge Newbery Airport, Buenos Aires, Argentina, Using TRSB/MLS Guidance. NASA Technical Memorandum 80223, January 1980.
5. Anon: TRSB Microwave Landing System Demonstration Program at Jorge Newbery Aeroparque, Buenos Aires, Argentina. FAA Report No. FAA-RD-14, 1978.
6. FAA Advisory Circular No. 120-29: Criteria for Approving Category I and Category II Landing Minima for FAR 121 Operations, September 1970.
7. FAA Advisory Circular No. 120-28B: Criteria for Approval of Category IIIa Landing Weather Minima, December 1977.
8. FAA Advisory Circular No. 20-57A: Automatic Landing Systems, January 1971.

TABLE I. - SUMMARY OF FLIGHT PERFORMANCE OF THE TCV B-737 AT
MONTREAL/DORVAL INTERNATIONAL AIRPORT USING
TRSB-MLS GUIDANCE.

DATE	(1) FLT/RUN	CONVENTIONAL-TO-MLS RNAV TRANSITION (ref. figures 11-13)		FINAL APPROACH, FIX (ref. figures 15,16)				CAT I DH (ref. figure 17)	
		Δ XTK,m	- Δ HER,m	XTK,m	-HER,m	Δ Y,m	Δ H,m	Δ y,m	Δ H,m
4/3/78	227A-2	87.8	- 87.8	3.7	0	8.6	1.8	-2.5	2.1
	227A-2R1	15.8	- 69.5	-14.6	-1.1	- 6.5	1.5	-1.8	0.6
	227A-5	-115.8	-118.3	20.7	1.2	- 8.1	3.0	0.3	0.5
	227B-2	273.1	- 47.5	- 4.9	1.2	3.4	3.2	-0.9	-0.4
4/5/78	227B-5	-146.3	- 74.4	26.8	1.2	14.1	2.8	4.3	0.1
	228A-2R1	208.5	- 26.8	7.3	-2.1	12.8	-0.3	-2.7	1.0
	228A-2R2	106.1	- 23.2	-17.1	-1.2	- 7.4	0.5	1.5	-0.1
	228A-5	- 79.2	- 51.2	8.5	-1.2	- 5.5	0.4	-2.7	-0.4
	228B-2	- 48.8	- 39.0	1.2	-2.0	8.9	-0.3	-0.5	0
	228B-5	-167.0	- 50.0	6.1	-2.2	- 8.9	0.5	2.0	0.3
	228B-6	30.5	- 35.4	- 8.5	2.4	4.3	3.5	-2.0	-1.1
	228B-7	- 58.5	- 39.0	- 2.4	-1.2	5.9	0.5	-2.6	-0.6
4/6/78	229A-2	14.6	- 48.8	- 8.5	-3.7	1.0	-1.6	-1.4	-0.1
	229A-2R1	- 32.9	- 57.3	1.2	0.7	6.2	2.1	-2.0	0.7
	229A-5	-237.7	- 59.7	18.3	1.7	3.3	3.4	-2.1	-5.4
	229B-2	-134.1	- 40.2	- 8.5	-2.4	- 2.0	-0.5	(2)	(2)
	229B-5	- 40.2	- 87.8	6.1	0	- 7.2	1.7	(2)	(2)
	229B-SR1	-128.0	- 89.0	6.1	0	- 4.9	2.2	(2)	(2)
	230A-2	-132.9	- 24.4	1.2	-0.2	6.8	1.3	-0.9	-0.5
	230A-2R1	197.5	- 47.5	- 4.9	0	5.2	1.8	-0.1	-0.9
4/7/78	230A-5	-106.1	- 62.2	+20.7	-1.2	9.0	0.8	-3.1	-1.6
	230B-2	90.2	- 19.5	- 8.5	-0.5	- 2.3	1.1	-1.2	-0.7
	230B-2R1	-187.8	- 26.8	-17.1	0	- 6.5	2.0	-0.3	0.3
	230B-5	-242.6	- 64.6	18.3	2.4	1.1	4.1	-3.6	0.9
	231A-5	-169.5	- 91.4	18.3	-1.2	(2)	(2)	(2)	(2)
	231A-SR1	- 71.9	- 89.0	14.6	-3.7	- 1.8	-1.6	(2)	(2)
	231A-SR2	- 65.8	- 91.4	12.2	-1.6	- 1.8	0	(2)	(2)
	231B-5	-145.1	- 76.8	8.5	0	- 6.6	2.0	1.6	-0.2
4/8/78	231B-SR1	- 65.8	- 82.9	6.1	1.6	- 8.8	3.5	0.4	-1.6
	231B-SR2	-103.6	- 86.6	- 3.7	-1.2	-16.2	1.2	-4.7	0
	232A-5	-201.2	- 35.4	2.4	-1.2	-14.4	1.2	1.1	-0.7
	232A-SR1	-215.6	- 37.8	- 3.7	-3.7	-15.8	-1.8	1.4	0.4
	232A-2	-142.6	- 36.6	-14.6	-1.2	- 4.8	0.2	1.1	0.3
	232B-5	-128.0	-46.3	6.1	-2.4	-10.4	-0.3	0.6	-0.1
	232B-SR1	-109.7	- 40.2	6.1	-3.7	-10.5	-1.7	1.5	-0.5
	232B-2	- 32.9	- 18.3	-11.0	-1.0	- 4.1	1.7	-0.1	-0.8
4/12/78	232C-5	-112.2	- 35.4	2.4	-4.9	- 7.7	-3.8	-0.5	1.6
	232C-SR1	121.9	- 42.7	- 6.1	-0.6	-21.1	1.2	1.9	0.8
	233-5	-212.1	- 7.3	- 3.7	1.2	-17.2	3.4	5.4	-1.0
	233-SR1	- 73.2	- 17.1	2.4	- 2.4	- 9.4	-0.5	0	1.1
	233-2	-115.8	1.2	-14.6	- 1.2	- 5.7	0.5	-5.9	-0.7
	234A-5	-264.6	- 57.3	6.1	1.2	- 8.9	3.5	-1.5	-0.2
	234A-SR1	-170.7	- 50.0	6.1	- 1.0	-11.3	1.5	-0.7	1.0
	234A-2	- 9.8	- 26.8	- 8.5	0	- 1.7	1.6	0.2	-0.4
4/14/78	234B-5	-182.9	- 59.7	26.8	0	9.9	1.7	-5.9	-0.5
	234B-SR1	-164.6	- 58.5	12.2	- 0.9	- 1.2	0.9	-3.1	0.2
	234B-2	- 64.6	- 30.5	- 4.9	- 0.5	-13.2	1.0	-0.1	0.5
	235A-5	-169.5	- 78.0	6.1	2.4	-10.4	4.3	(2)	(2)
	235A-SR1	-193.9	- 67.1	- 6.1	0	(3)	1.2	---	---
	235A-2	-225.6	- 64.6	- 8.5	- 0.6	2.9	1.2	(2)	(2)
	235B-5	-260.9	- 81.7	0	- 1.0	-13.8	1.2	2.9	0.1
	235B-SR1	- 87.8	- 74.4	4.9	- 1.2	-11.7	0.5	2.5	-0.2
4/15/78	235B-2	-185.3	- 63.4	- 2.4	0	4.2	1.8	-0.3	0.1
	236A-5	-160.5	- 61.0	8.5	2.4	- 3.4	4.3	-3.2	0.7
	236A-SR1	-203.6	- 39.0	8.5	0	- 4.4	1.9	-1.9	0.1
	236A-2	- 75.6	- 29.3	- 8.5	- 2.3	1.1	-0.8	-0.9	-1.0
	236B-5	-187.8	- 57.3	0	- 1.2	-14.5	0.9	1.2	0.6
	236B-SR1	-130.5	- 59.7	24.4	0	10.4	2.0	-2.3	-1.5
	236B-2	-207.3	- 34.1	- 8.5	- 2.0	1.7	0.2	-0.1	1.6
	Mean	- 95.3	- 52.8	2.2	- 0.7	- 3.3	1.2	-0.6	-0.1
Est. Standard Deviation		\pm 117.7	\pm 24.5	\pm 11.0	\pm 1.6	\pm 8.3	\pm 1.6	\pm 2.3	\pm 1.1

*Notes:

- (1) Run = 2 refers to STAR DORA 2, = 5 refers to STAR DORA 5.
- (2) Unavailable due to formatter malfunction and switch to flare data group in PCM data.
- (3) Unavailable - formatter malfunction, Δ y limited - no localizer capture.
- (4) NCU data ended before flare initiation.

CAT II DH (ref. figure 18)		FLARE INITIATION (ref. figure 19)		WINDS @ FLARE	TOUCHDOWN (ref. figure 21)			REMARKS
$\Delta y, m$	$\Delta H, m$	$\Delta y, m$	$\Delta H, m$		$\Delta y, m$	R Rhumb, III	hMLS, m/s	
-1.2 1.1 -2.0	-2.4 -0.1 -1.7	-2.7 1.3 -2.8	-1.9 -1.7 -0.1	2703 2506 2609	-2.1 -1.0 -4.9	- 51.8 - 46.7 -117.0	-0.53 -0.85 -1.01	USING ILS DME USING ILS DME USING ILS DME
-0.1 1.4	1.4 -0.2	2.3 -0.4	0.1 0.1	2604 2803	0.6 -4.3	- 5.9 -104.8	-0.73 -0.67	USING ILS DME USING ILS DME
-3.8 2.8 3.2	-0.2 0.4 0.9	-2.2 1.0 3.2	-1.4 -0.1 -1.2	2624 2725 2729	-2.7 1.5 2.7	+ 25.1 - 39.4 25.4	-0.89 -1.07 -1.20	USING ILS DME USING ILS DME USING ILS DME
-2.5 2.7 -2.3 -2.9	-2.2 -0.6 0.8 0.2	-3.8 0.3 -3.2 -2.9	-1.0 0.6 -0.2 1.0	2720 2723 2721 2720	-3.1 -0.2 -0.8 -1.9	- 70.0 - 75.3 - 1.7 - 29.0	-0.81 -1.18 -1.16 -0.87	STAR DORA 2 STAR DORA 2
1.4 0.9 -3.7	0.5 0.5 -2.0	1.7 -2.2 -3.8	0.3 1.6 -1.3	2710 2710 2714	2.9 -0.7 -4.1	- 76.6 -115.9 - 51.4	-1.03 -0.65 -0.82	
(2) (2) (2)	(2) (2) (2)	(2) (2) (2)	(2) (2) (2)	2716 2616 2615	(2) (2) (2)	-160.5 - 86.0 - 67.5	-1.16 -0.95 -0.87	
-0.4 -2.3 -3.9	1.3 1.2 0.3	-1.2 -2.2 -4.8	1.2 0.4 0.2	3601 2703 0402	-1.1 -2.7 -3.1	-161.7 - 37.5 -108.5	-0.73 -0.87 -0.37	
0.5 0.9 -0.9	-0.4 0.5 -0.1	-0.2 0.8 -1.9	-0.2 -0.1 0.9	2604 2705 2713	-0.7 0.8 -2.9	-140.8 -120.2 - 68.1	-0.60 -0.63 -0.76	
(2) (2) (2)	(2) (2) (2)	(2) (2) (2)	(2) (2) (2)	2726 2624 2729	(2) (2) (2)	- 52.2 -123.6 - 20.0	-0.93 -1.04 -0.94	
1.6 -0.3 2.3	0.1 0.1 -0.8	1.2 1.8 0.5	0.4 0.2 0.5	2624 2623 2619	0.5 -0.3 0.1	- 43.5 - 87.8 - 59.4	-1.07 -0.99 -0.65	
0.2 2.4 -1.8	0.9 -0.5 -0.8	1.2 1.5 -0.5	0.7 -0.4 -0.6	2622 2717 2617	0.2 0 -2.6	- 53.5 - 76.3 - 36.4	-1.08 -0.99 -1.19	
2.0 0.2 1.0	1.3 -0.3 0.4	0.4 0 2.0	-0.7 -0.7 0.4	2715 2712 2620	-1.6 -0.5 0.1	- 15.0 - 80.6 -132.0	-1.17 -1.16 -0.69	
0.5 2.7	1.6 -0.2	0.5 2.1	2.3 0.1	2712 (4)	-0.7 0.7	- 97.5 -102.1	-1.16 -0.97	
4.9 3.4 -1.6	-0.2 -1.6 -0.7	3.1 0.2 -1.7	0.3 -1.2 0.3	0000 3403 2603	2.0 0.5 0	-127.5 -163.9 -138.1	-0.80 -0.81 -0.88	
0 0.3 0.2	0.7 0.2 0.3	-0.5 0.5 -1.3	-0.3 0.6 0.6	2719 2720 2717	1.0 0.1 -0.3	- 56.8 -106.5 -133.7	-1.01 -0.93 -0.71	
-4.5 -0.3 0	-0.1 -1.1 0.5	-2.6 -1.0 -2.2	0.5 -1.4 -0.6	2624 2720 2718	-2.8 -2.4 -2.0	-110.0 -116.6 - 87.0	-0.86 -0.81 -0.86	
(2) ----- (2)	(2) ----- (2)	(2) ----- (2)	(2) ----- (2)	2723 ----- 2721	(2) ----- (2)	- 56.0 ----- - 75.7	-0.95 ----- -1.09	NO LOCALIZER CAPTURE
-0.1 1.6 -0.3	0.4 -0.2 0.7	3.0 0.9 -1.3	1.2 -0.3 0.3	2721 2722 2622	0.4 0.2 -0.5	- 71.6 - 86.8 - 68.2	-0.81 -0.94 -0.88	
-0.3 -0.5 0.2	0.2 0 0.3	-1.6 -1.7 0	-0.1 0.1 0.4	2510 2510 2611	-1.9 -1.6 -0.5	-161.7 - 80.0 - 42.3	-0.87 -0.65 -0.89	
3.3 -4.1 2.7	-0.7 -0.8 -0.3	1.7 -2.4 0.9	-0.5 -1.6 -0.3	2605 2611 2837	-0.7 -3.5 -0.2	- 99.0 - 29.8 -170.2	-0.59 -1.03 -0.79	
0.1 ± 2.2	-0.1 ± 0.9	-0.4 ± 2.0	-0.1 ± 0.9	2715 ± 7	-0.9 ± 1.7	- 80.1 ± 46.5	-0.89 ± 0.19	



Figure 1. - NASA TCV B-737 Research Aircraft.

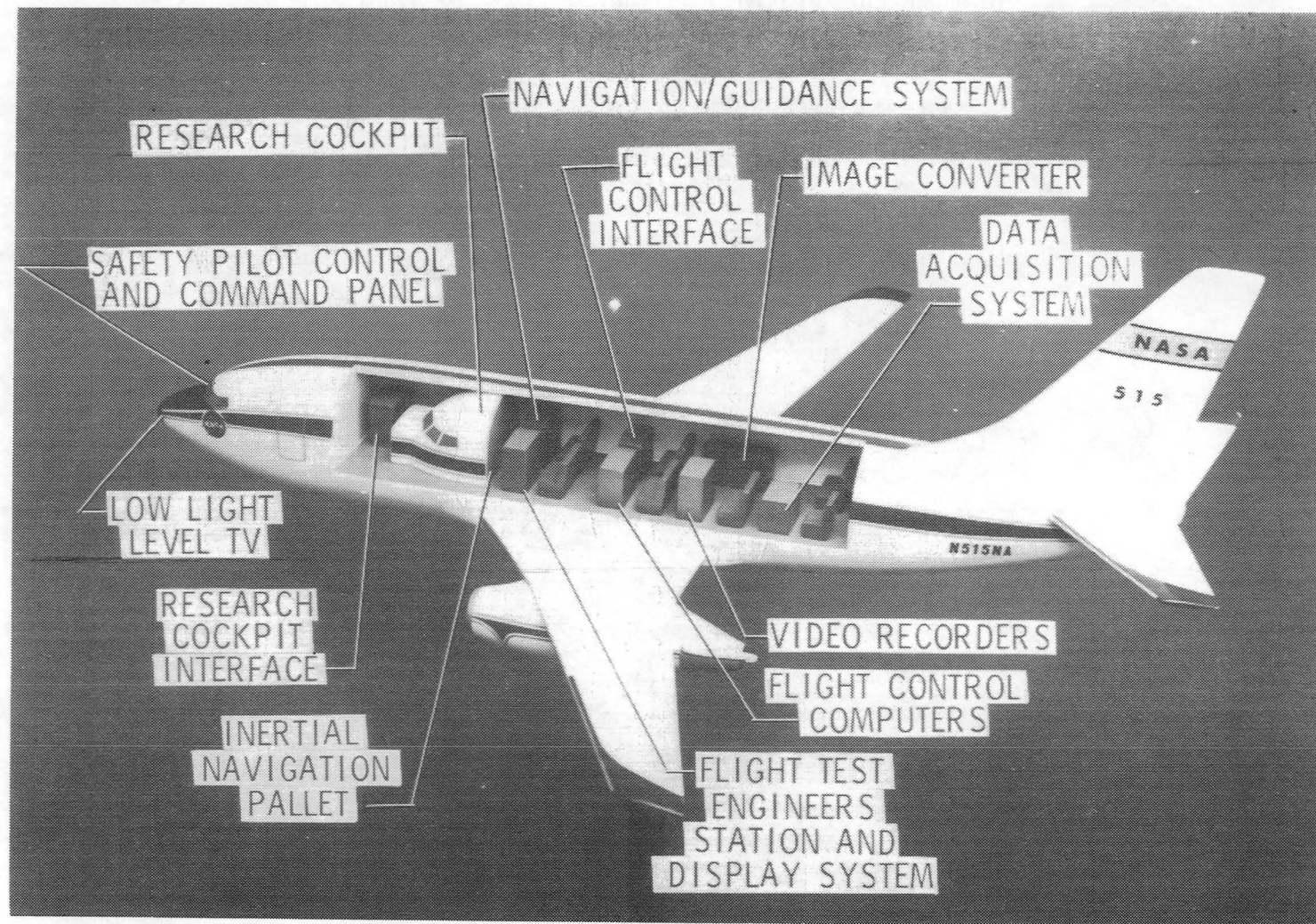


Figure 2. - NASA TCV B-737 Research Aircraft (Internal Arrangement).

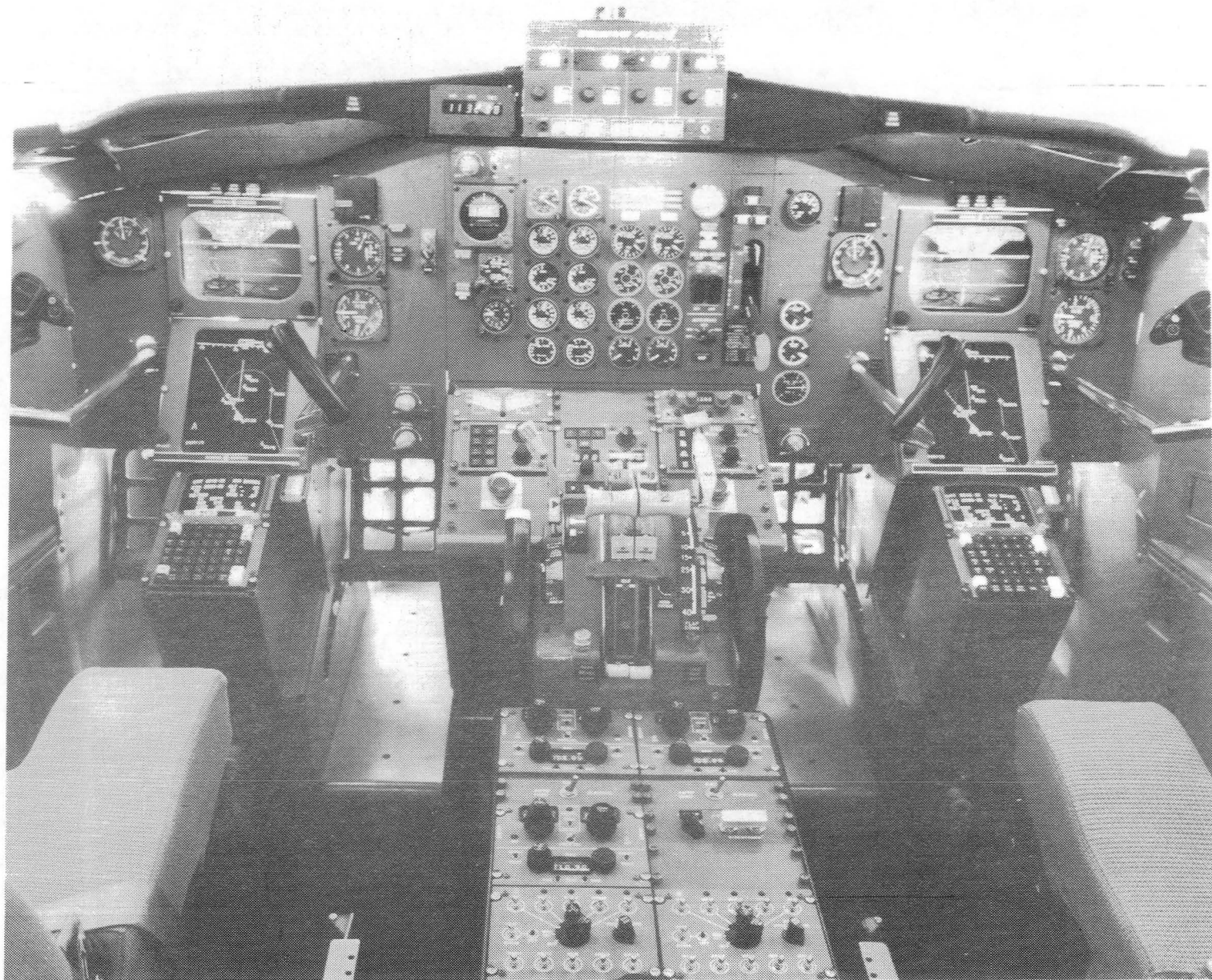


Figure 3. - Aft Flight Deck Display Arrangement.

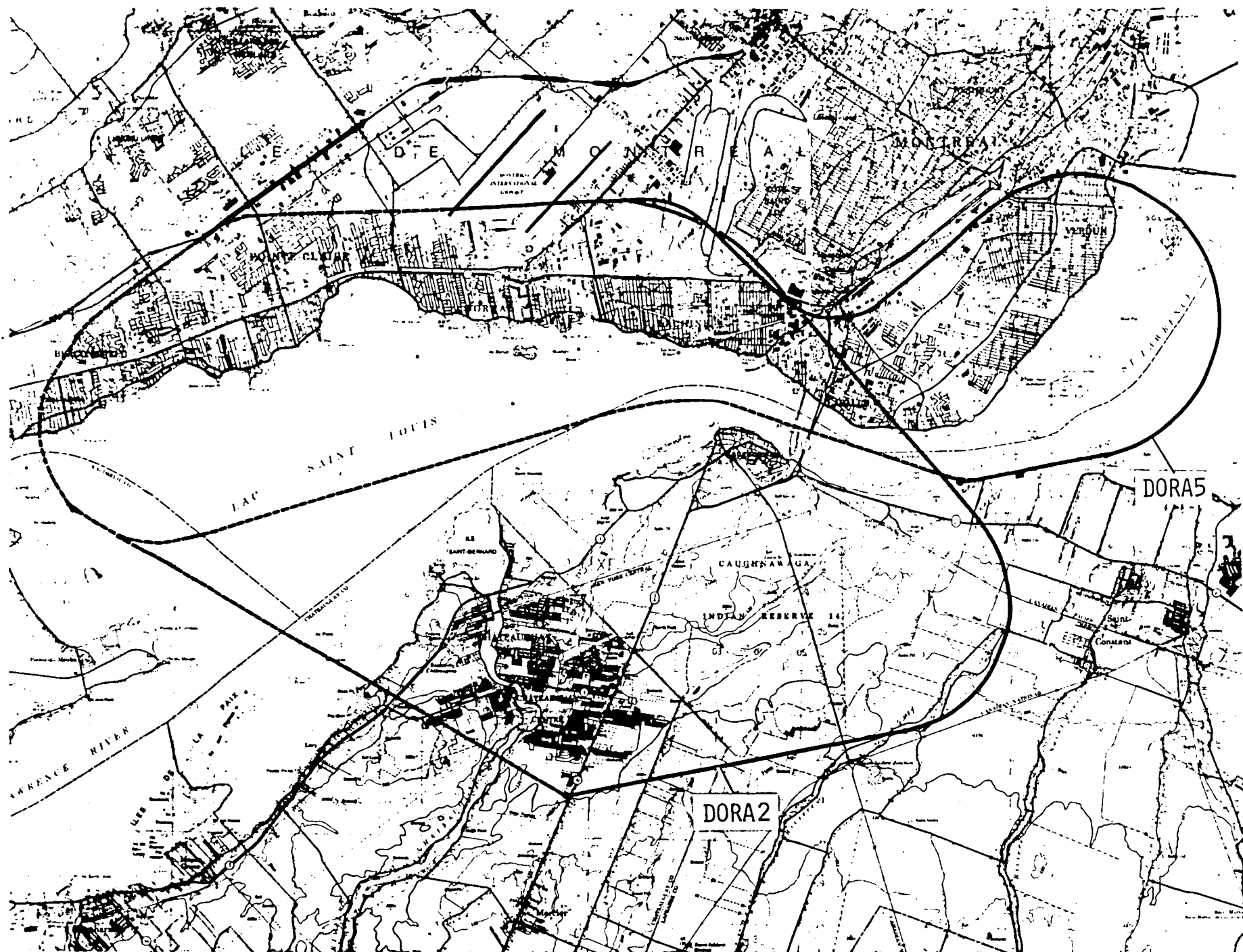


Figure 4. - Approach Paths used by TCV B-737 at Montreal/Dorval International Airport, Montreal, Canada.

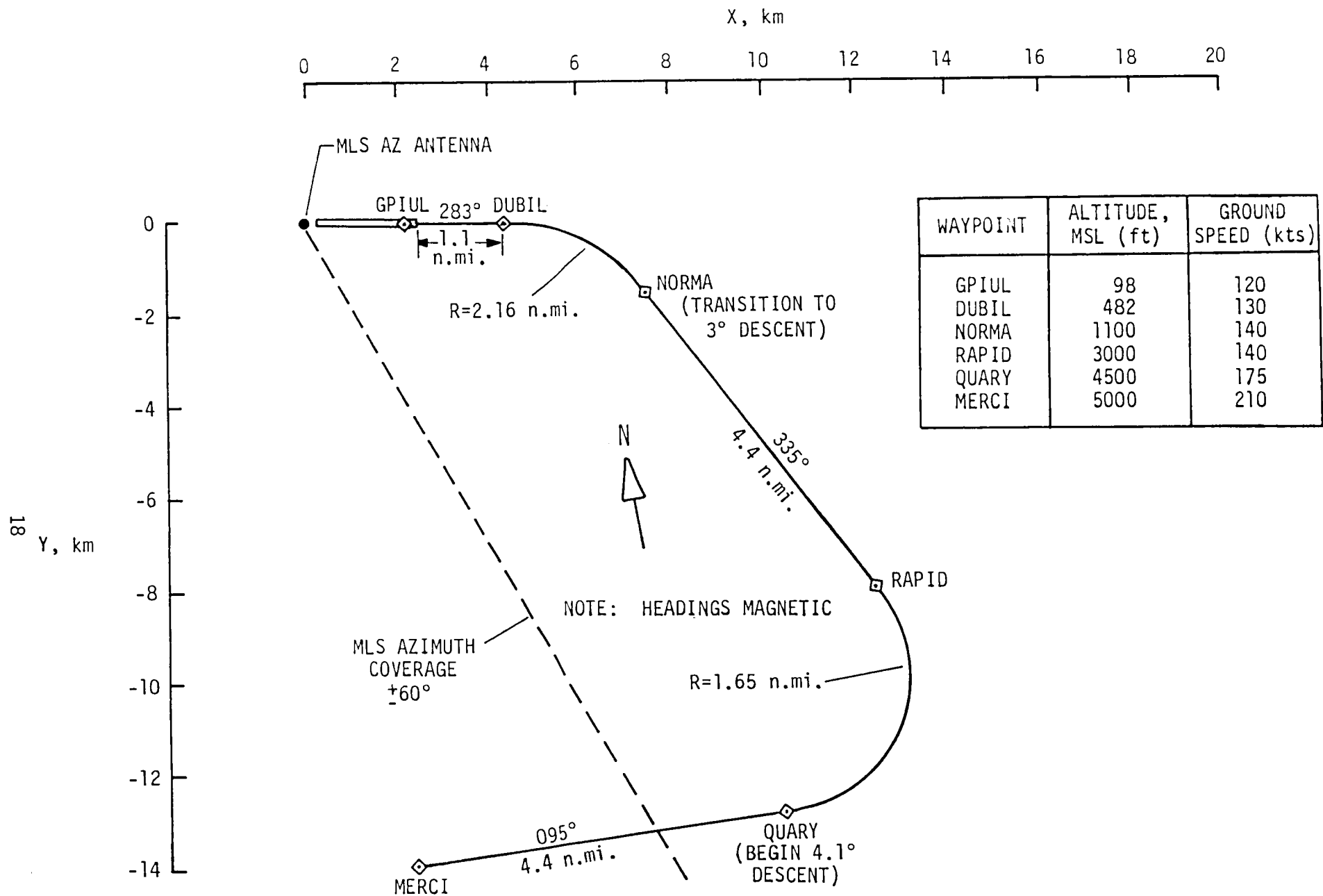


Figure 5. - Standard Terminal Arrival Route DORA2 to Montreal/Dorval International Airport.

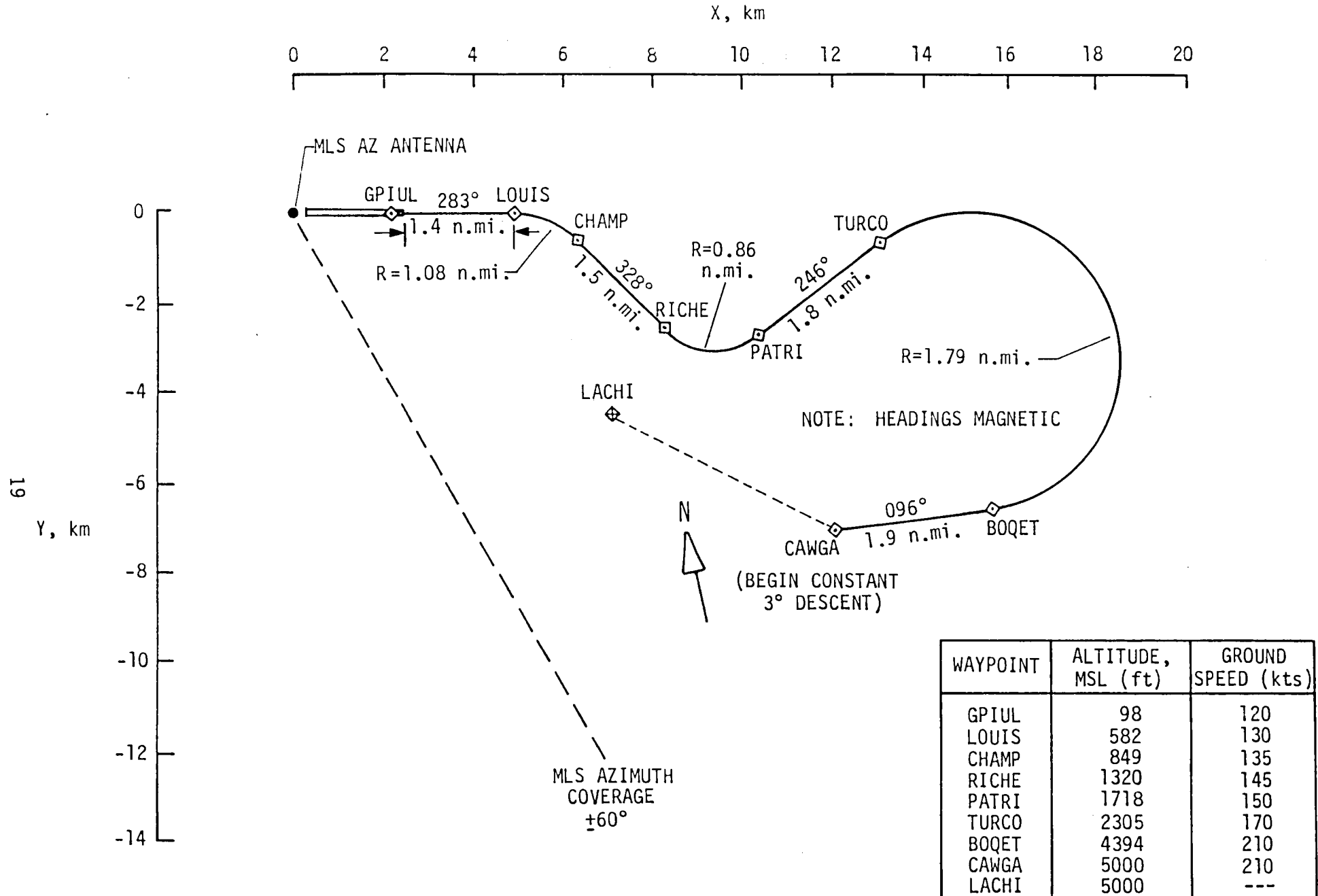
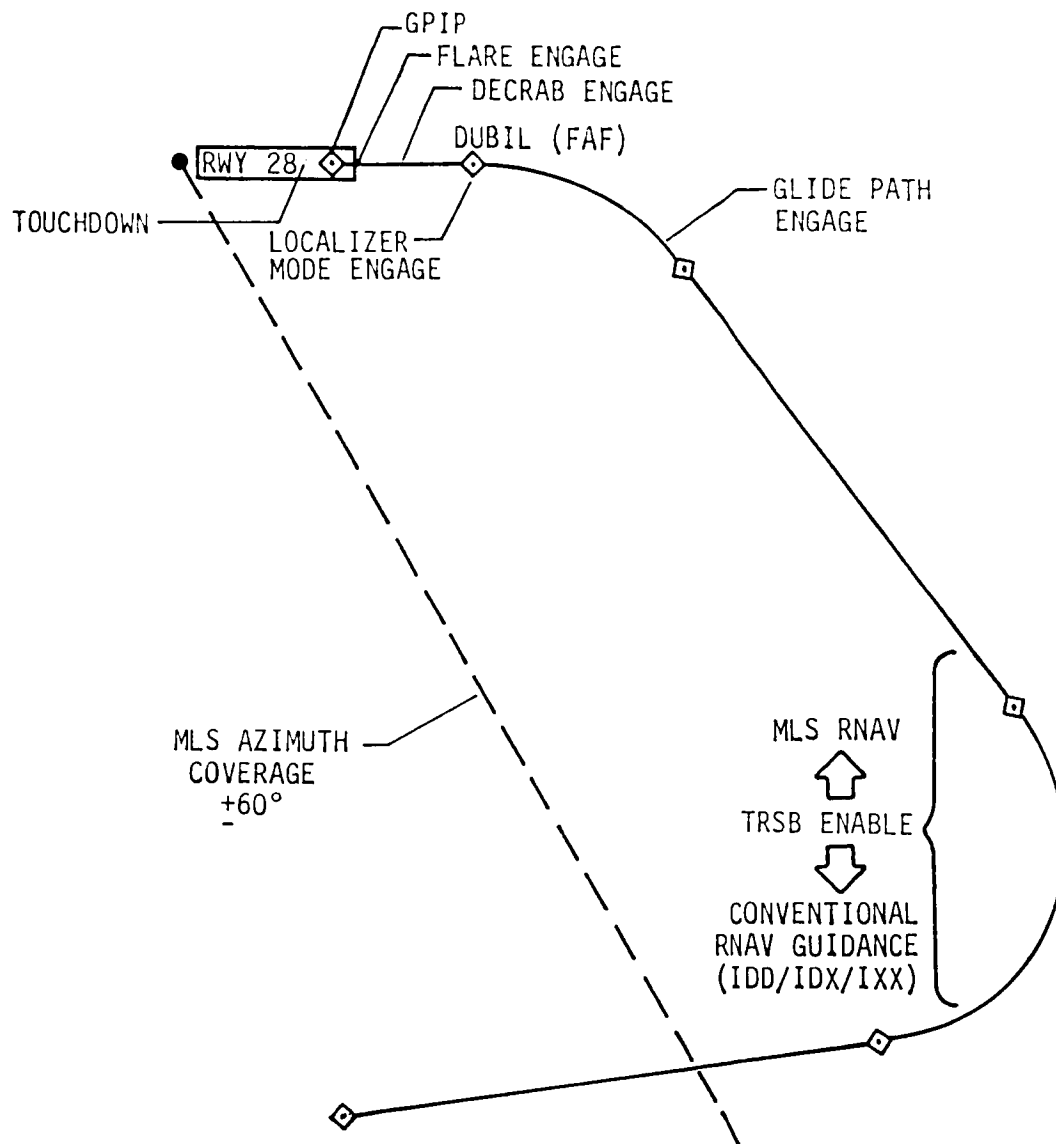
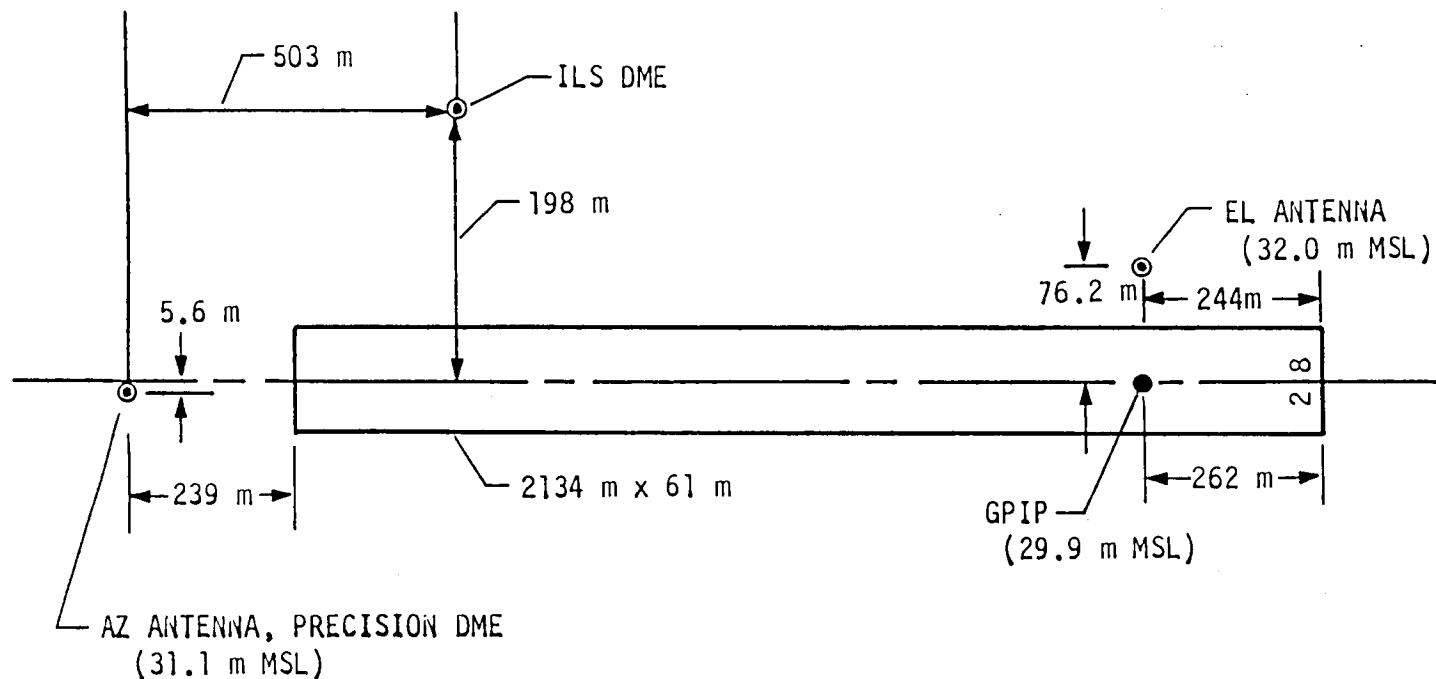


Figure 6. - Standard Terminal Arrival Route DORA5 to Montreal/Dorval International Airport.



EVENT	CONTROL LAW	
	LATERAL	LONGITUDINAL
TRSB ENABLE	RNAV	RNAV
GLIDE PATH ENGAGE	RNAV	AUTOLAND: GLIDE PATH TRACK
LOC. MODE ENGAGE	AUTOLAND: LOCALIZER TRACK	AUTOLAND: GLIDE PATH TRACK
DECRAB ENGAGE	AUTOLAND: DECRAB/ROLLOUT	AUTOLAND: GLIDE PATH TRACK
FLARE ENGAGE	AUTOLAND: DECRAB/ROLLOUT	AUTOLAND: FLARE/ROLLOUT

Figure 7. - TCV B-737 Control Law Schedule for Montreal/Dorval International Automatic MLS Approaches and Landings.



RUNWAY TRUE HEADING: 267.65°

AZ ANTENNA COORDINATES: 45°27'45.03" N, 73°46'9.32" W

GPIP COORDINATES: 45°27'48.03"N, 73°44'32.27" W

NOTE: DRAWING NOT TO SCALE

Figure 8. - MLS Configuration for Runway 28 at Montreal/Dorval International Airport.

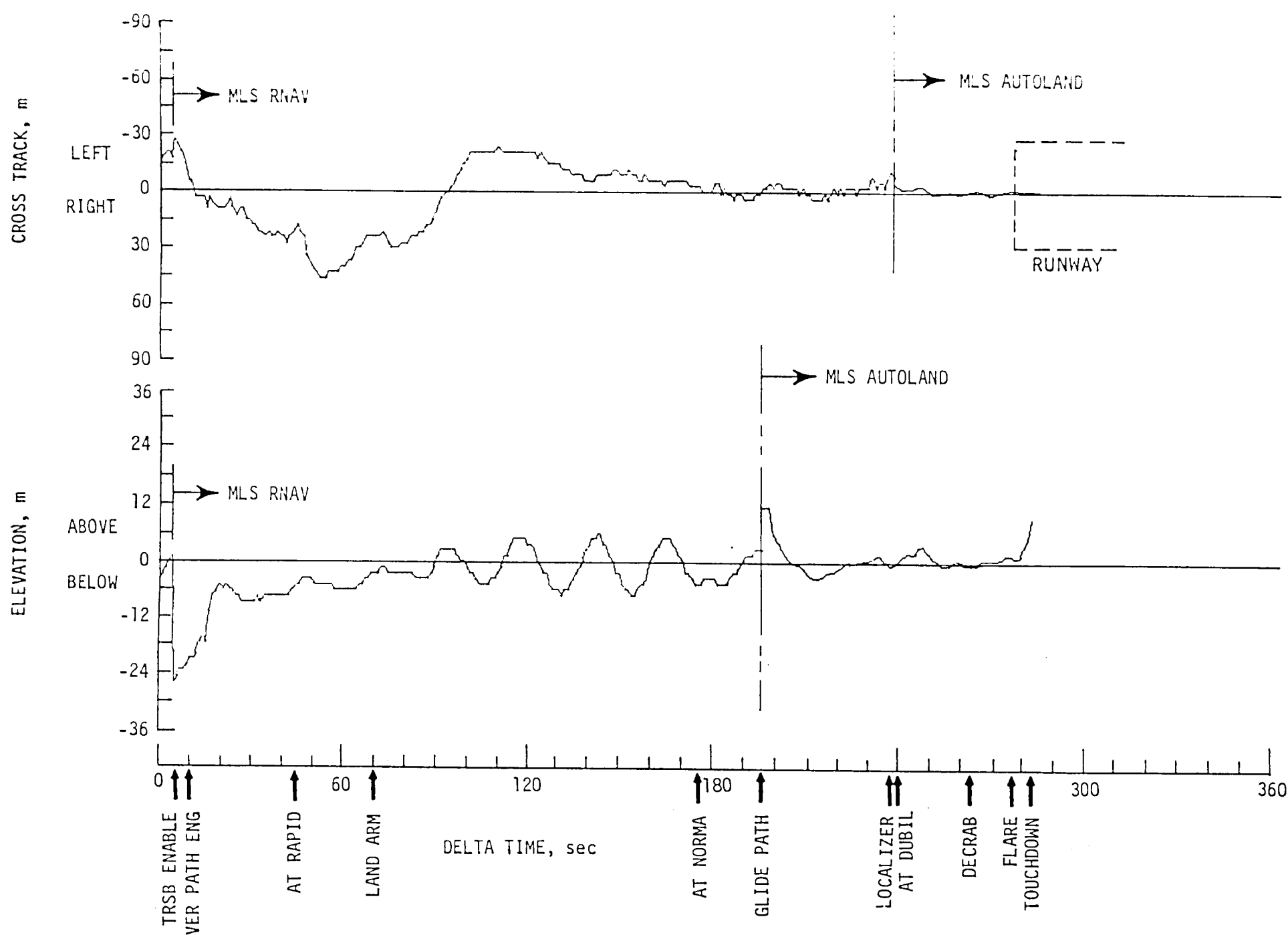


Figure 9. - Flight Technical Errors for Typical DORA2 Automatic MLS Approach at Montreal/Dorval International (Flight/Run No. 234A-2).

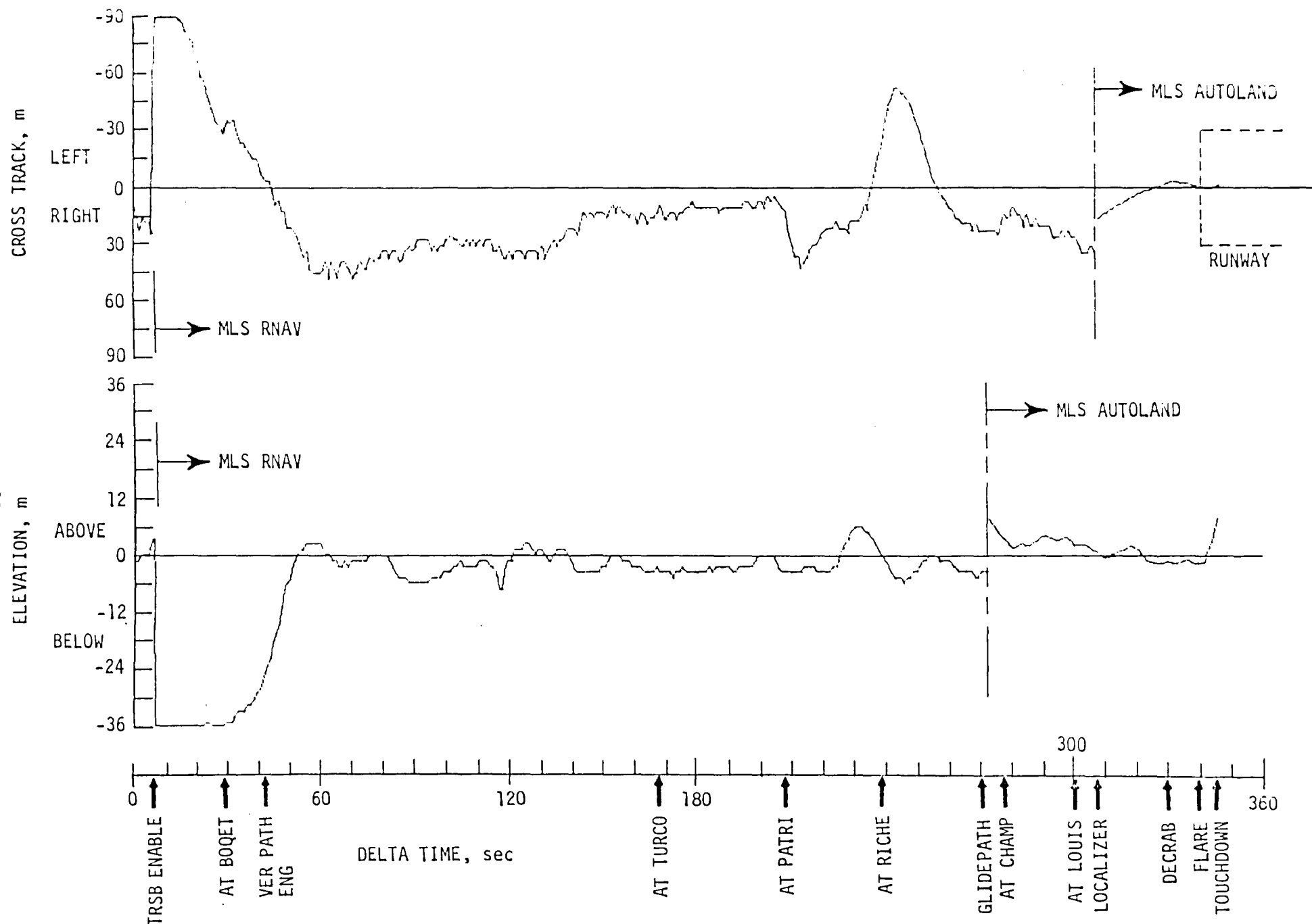


Figure 10. - Flight Technical Errors for Typical Dora 5 Automatic MLS Approach at Montreal/Dorval International (Flight/Run No. 235B-5R1).

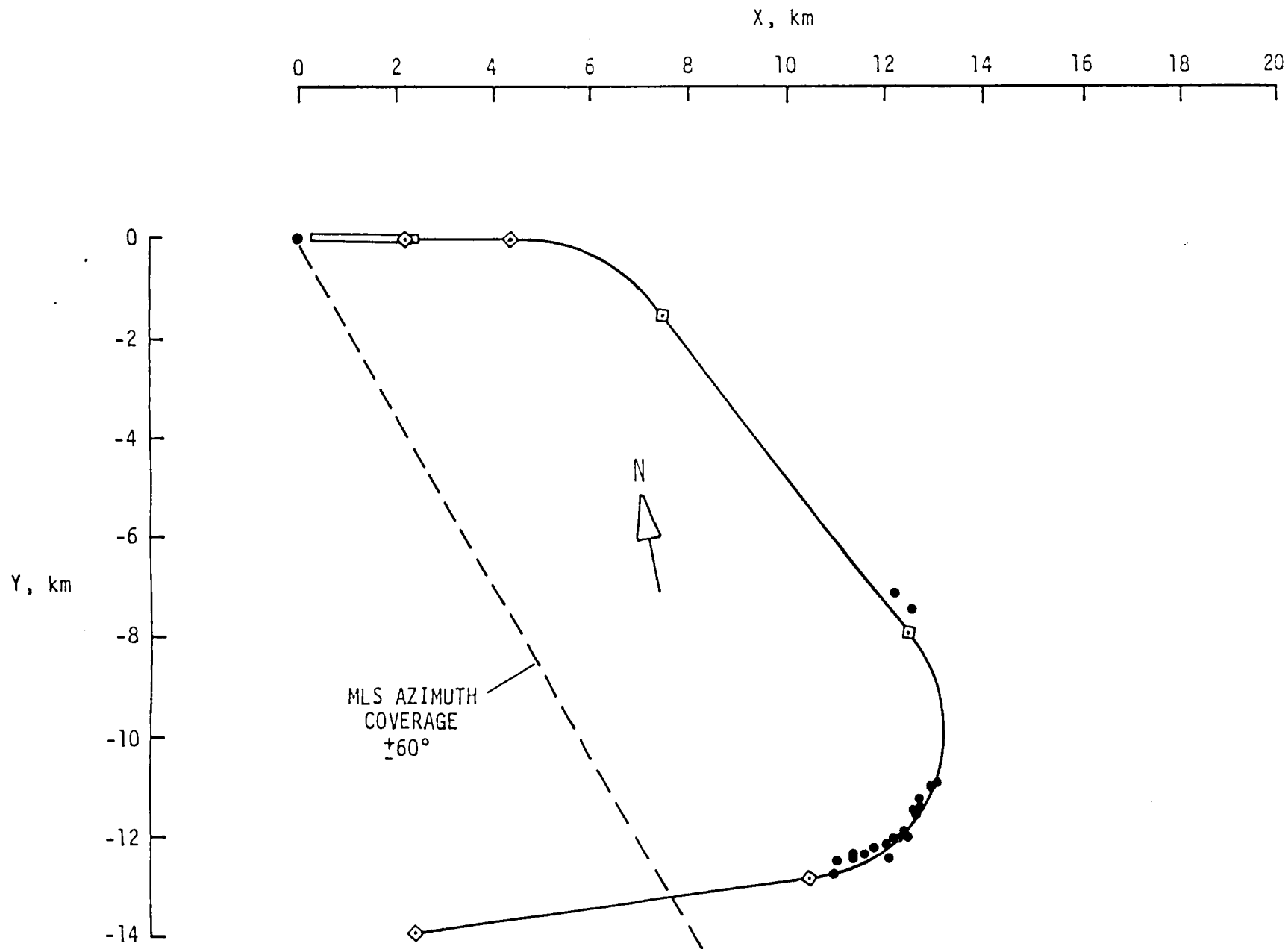


Figure 11. - Summary of Conventional-to-MLS RNAV Lateral Path Offsets for
TCV B-737 Approaches to Montreal/Dorval International on DORA2.

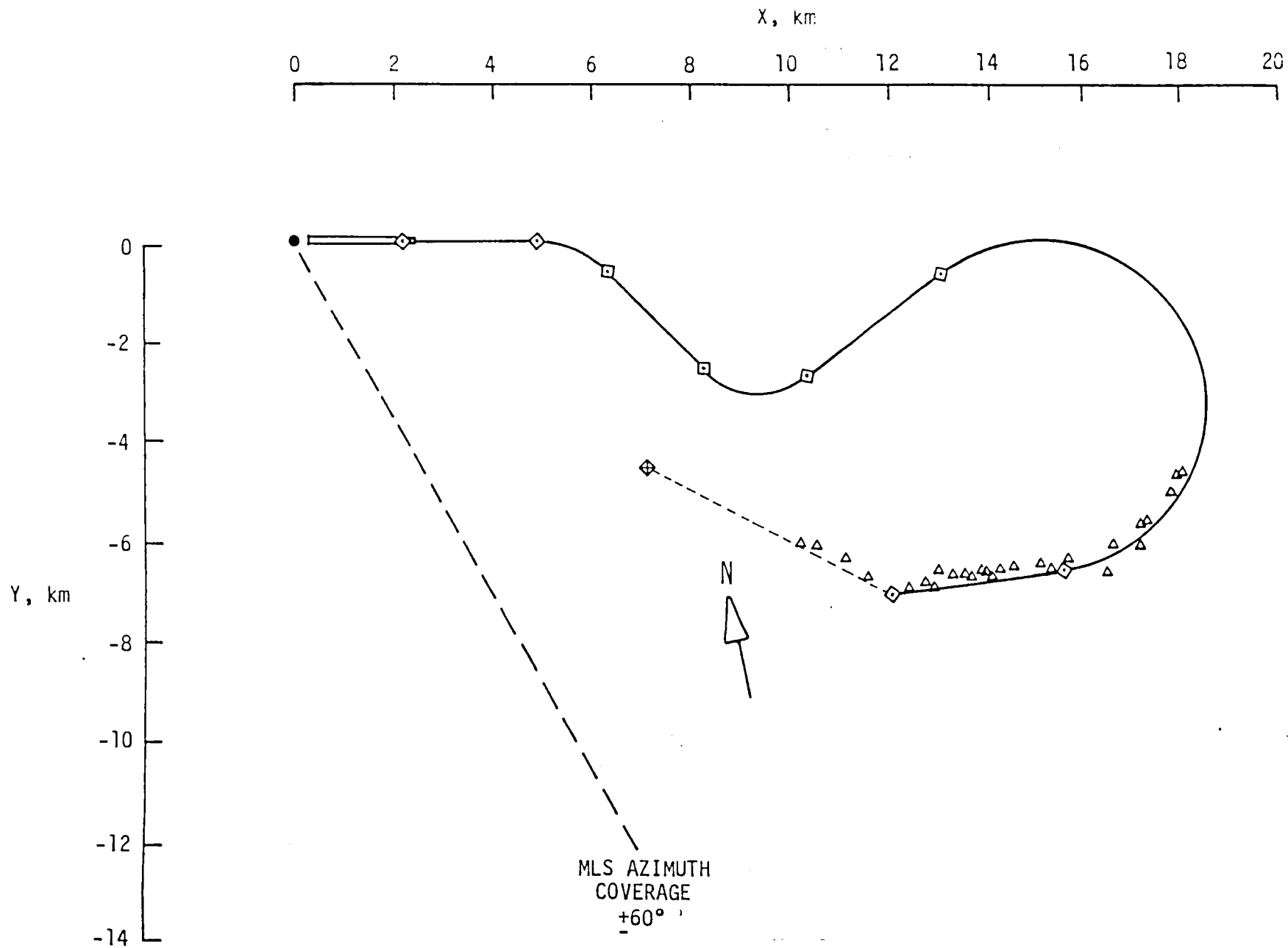


Figure 12. - Summary of Conventional-to-MLS RNAV Lateral Path Offsets for TCV B-737 Approaches to Montreal/Dorval International on DORA5.

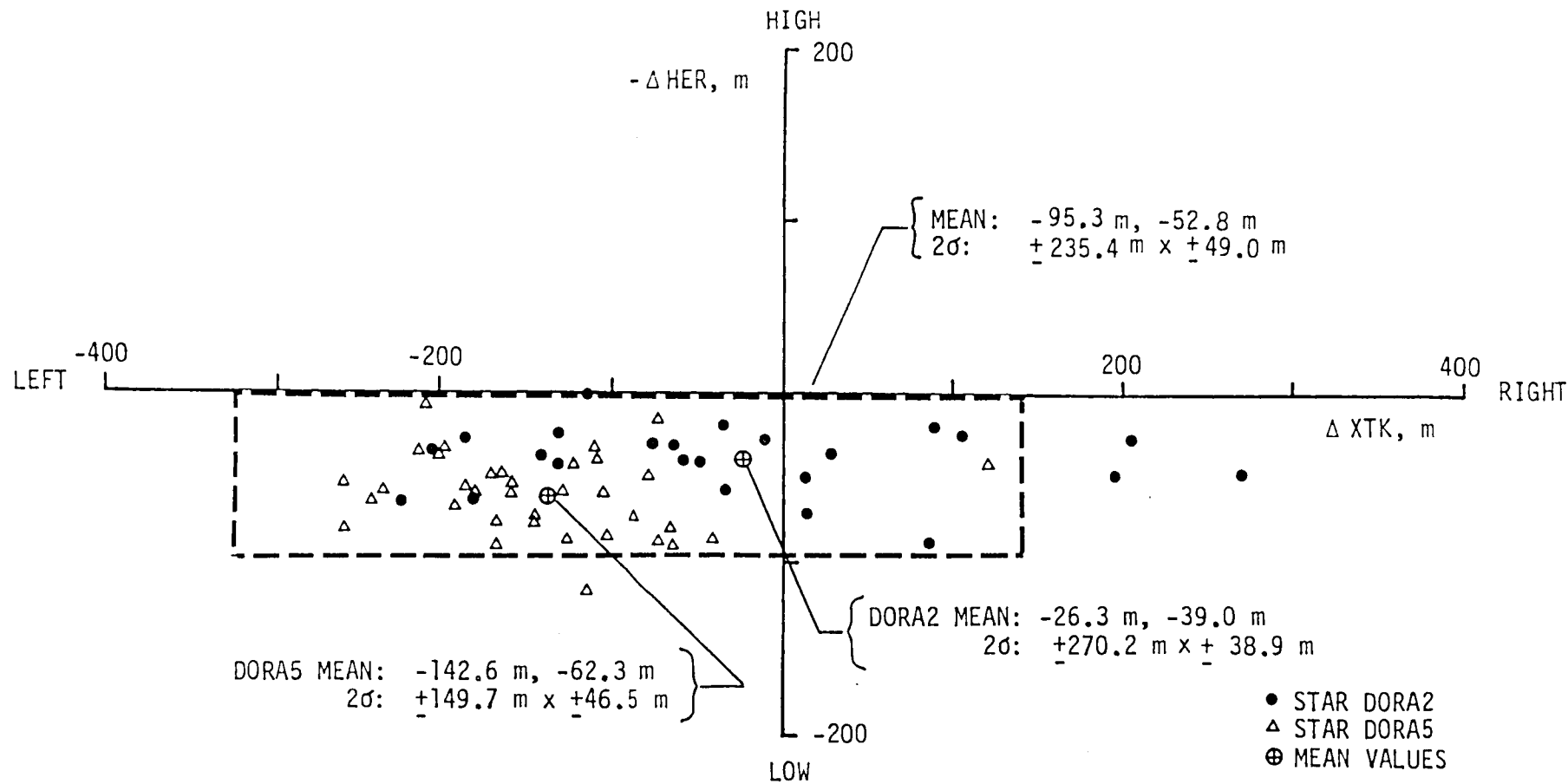


Figure 13. - Summary of $-\Delta \text{HER}$ Versus ΔXTK at Conventional-to-MLS RNAV Transition for Montreal/Dorval International Automatic MLS Approaches.

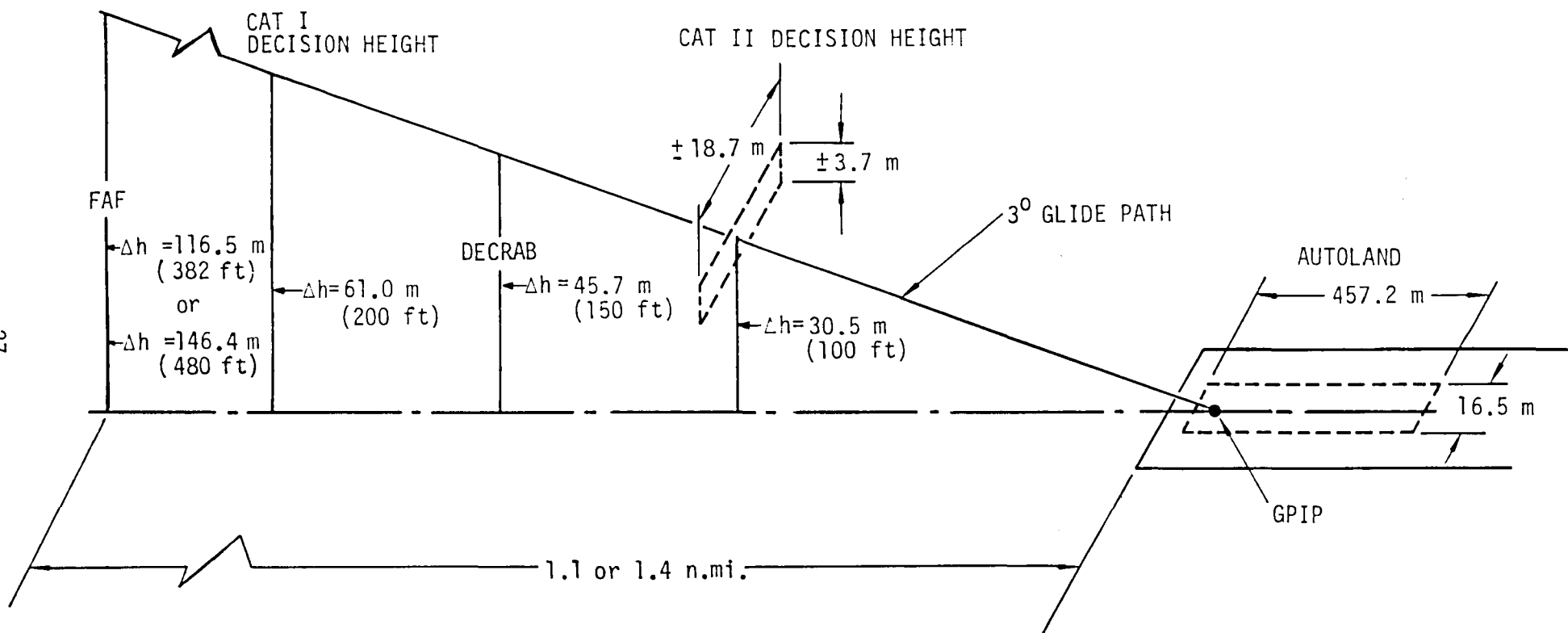


Figure 14. - Montreal/Dorval International Approach and Landing Profile Showing FAA Criteria (2d) for Automatic Systems (see references 6, 7, and 8).

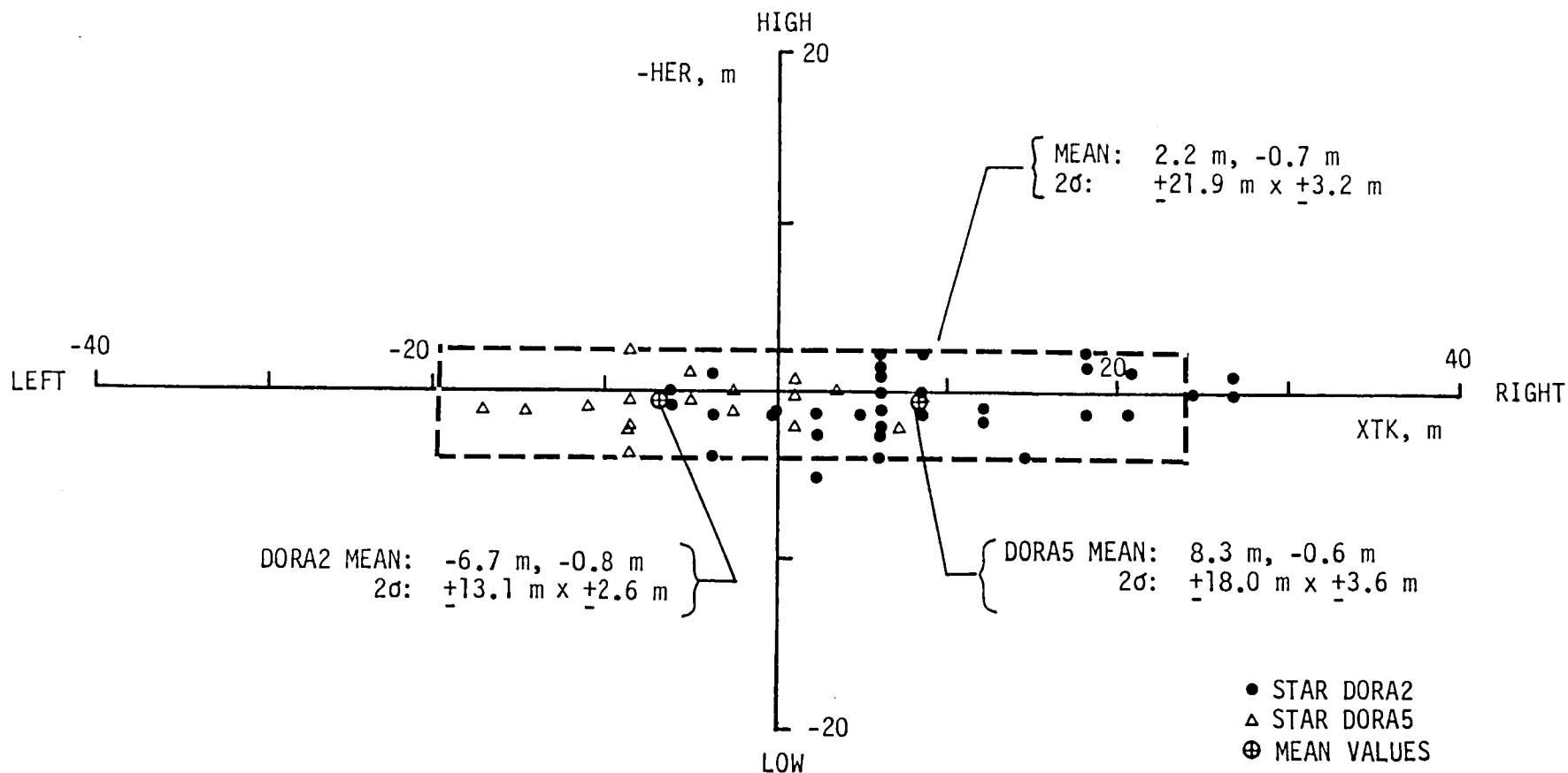


Figure 15. - Summary of -HER versus XTK at the Final Approach Fix for Montreal/Dorval International Automatic MLS Approaches.

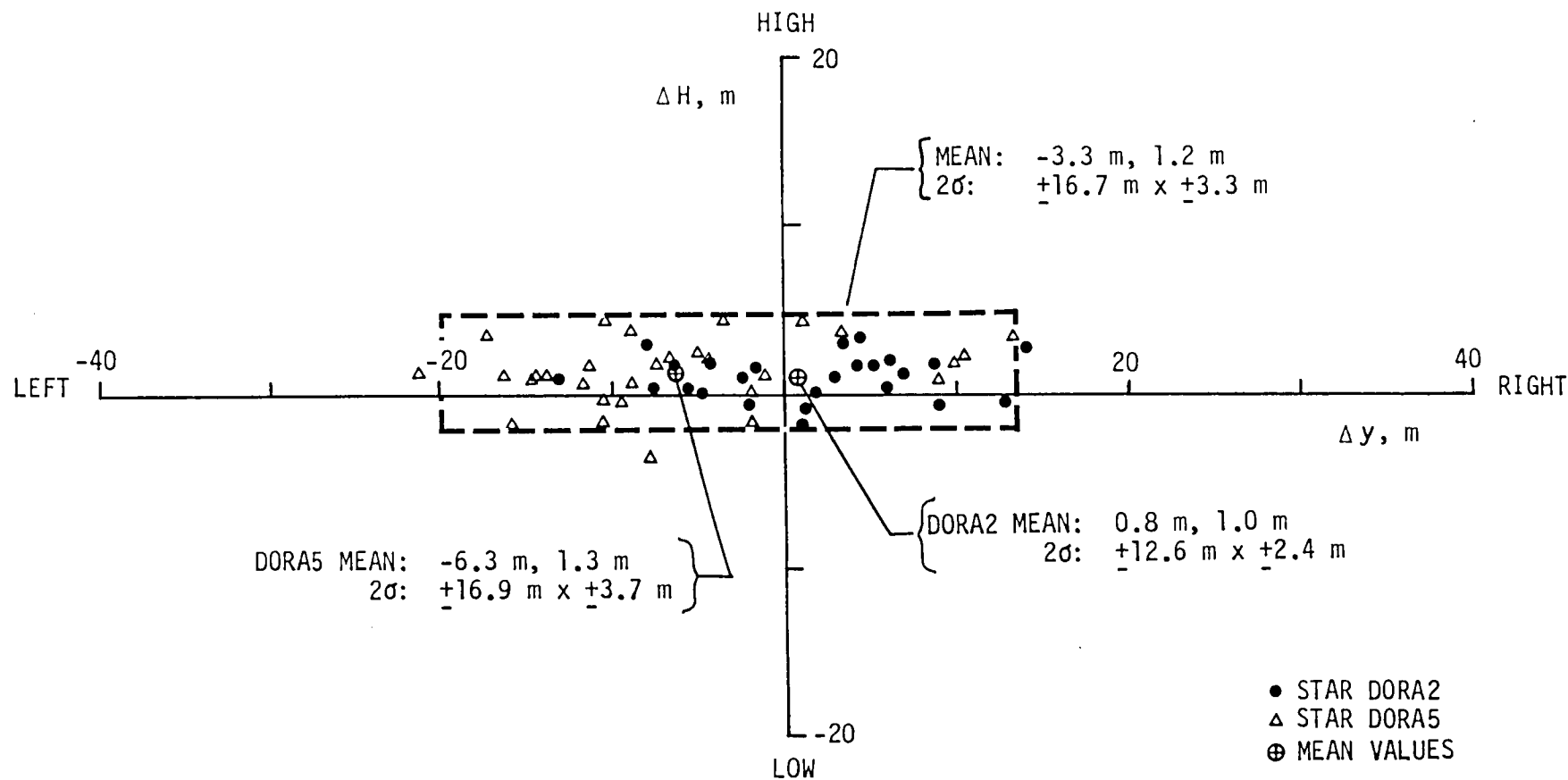


Figure 16. - Summary of TRSB - Derived Errors at the Final Approach Fix for Montreal/Dorval International Automatic MLS Approaches.

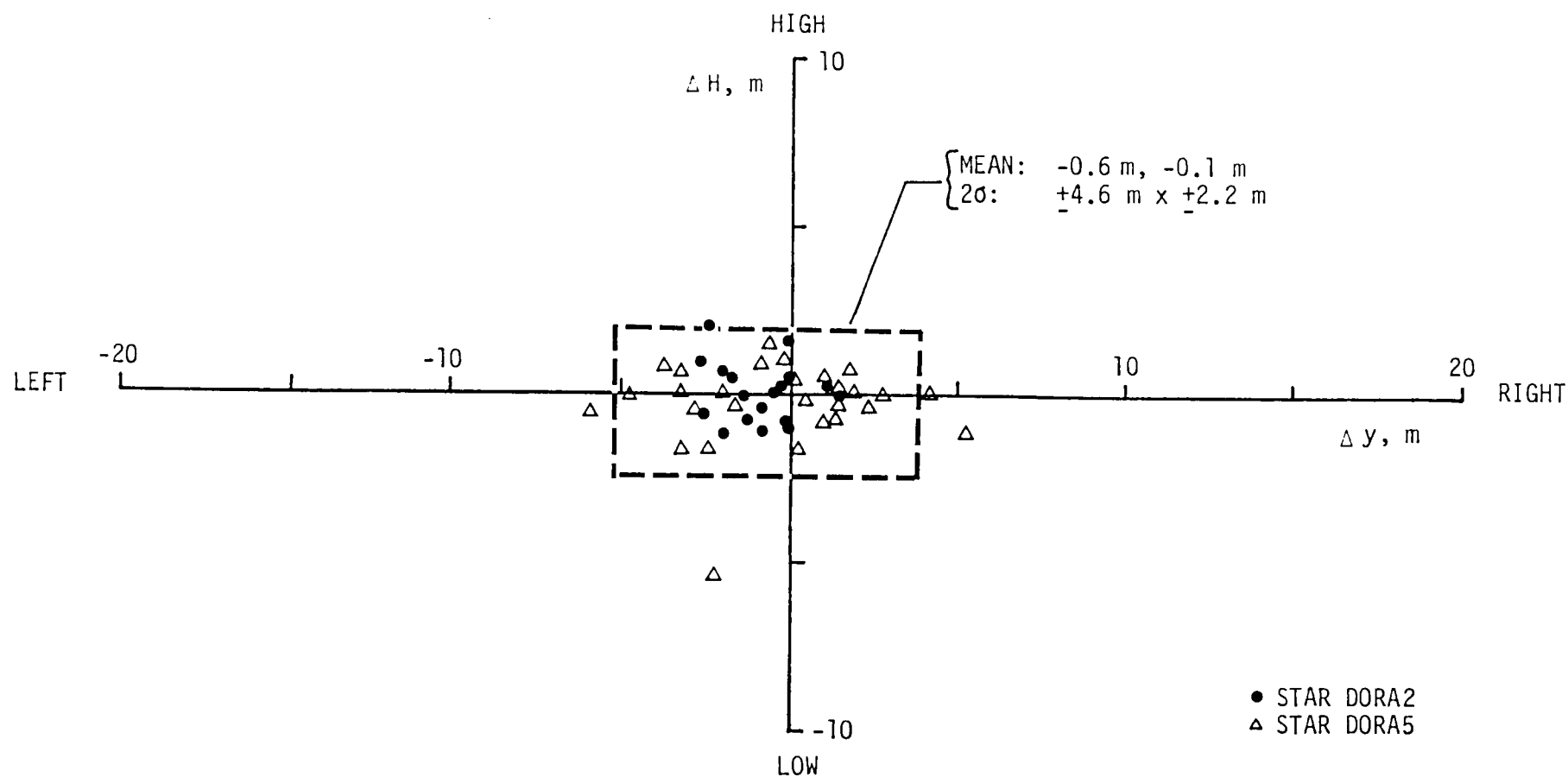


Figure 17. - Summary of TRSB - Derived Errors at the CAT I Decision Height for Montreal/Dorval International Automatic MLS Approaches.

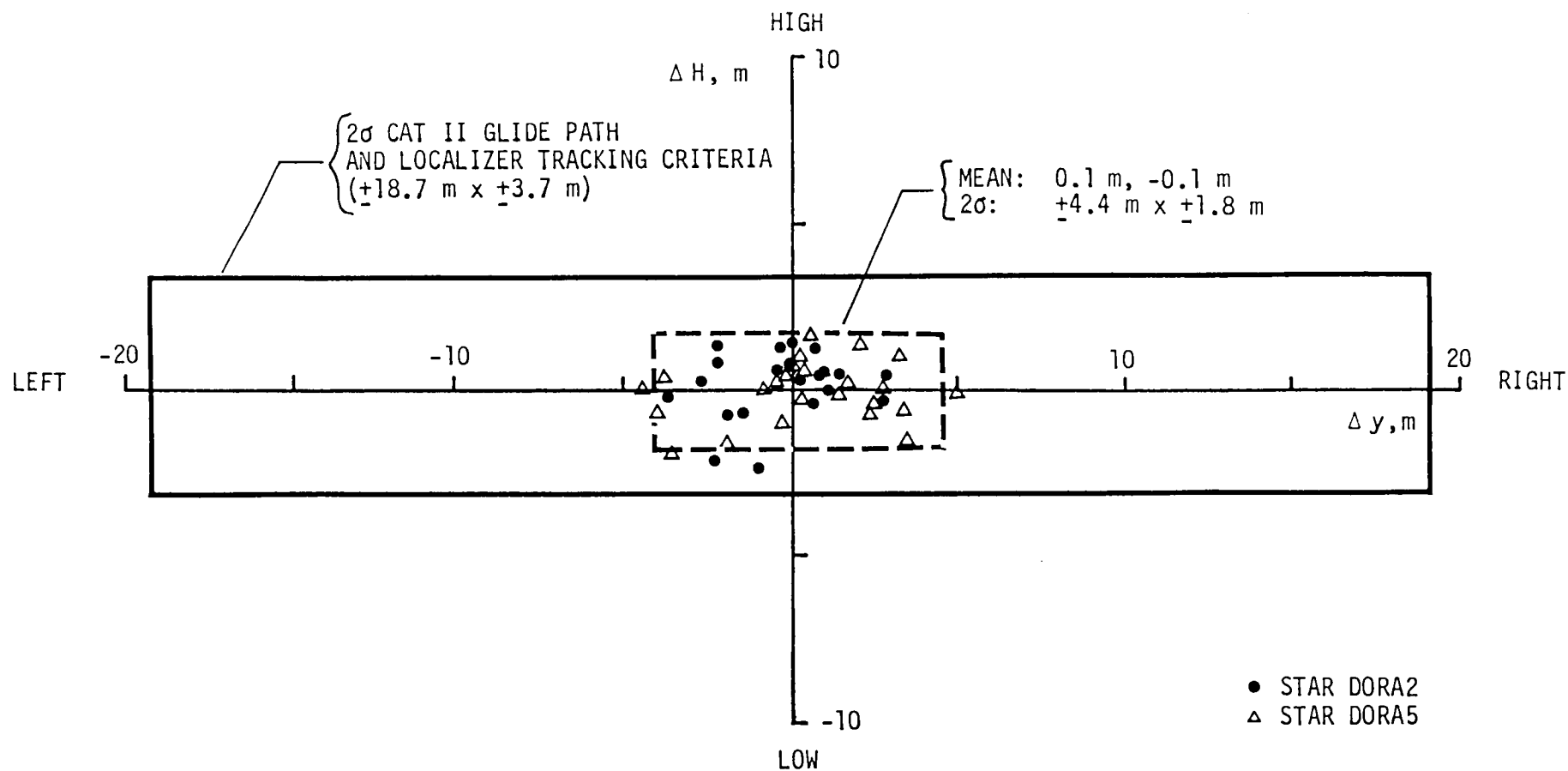


Figure 18. - Summary of TRSB - Derived Errors at the CAT II Decision Height for Montreal/Dorval International Automatic MLS Approaches.

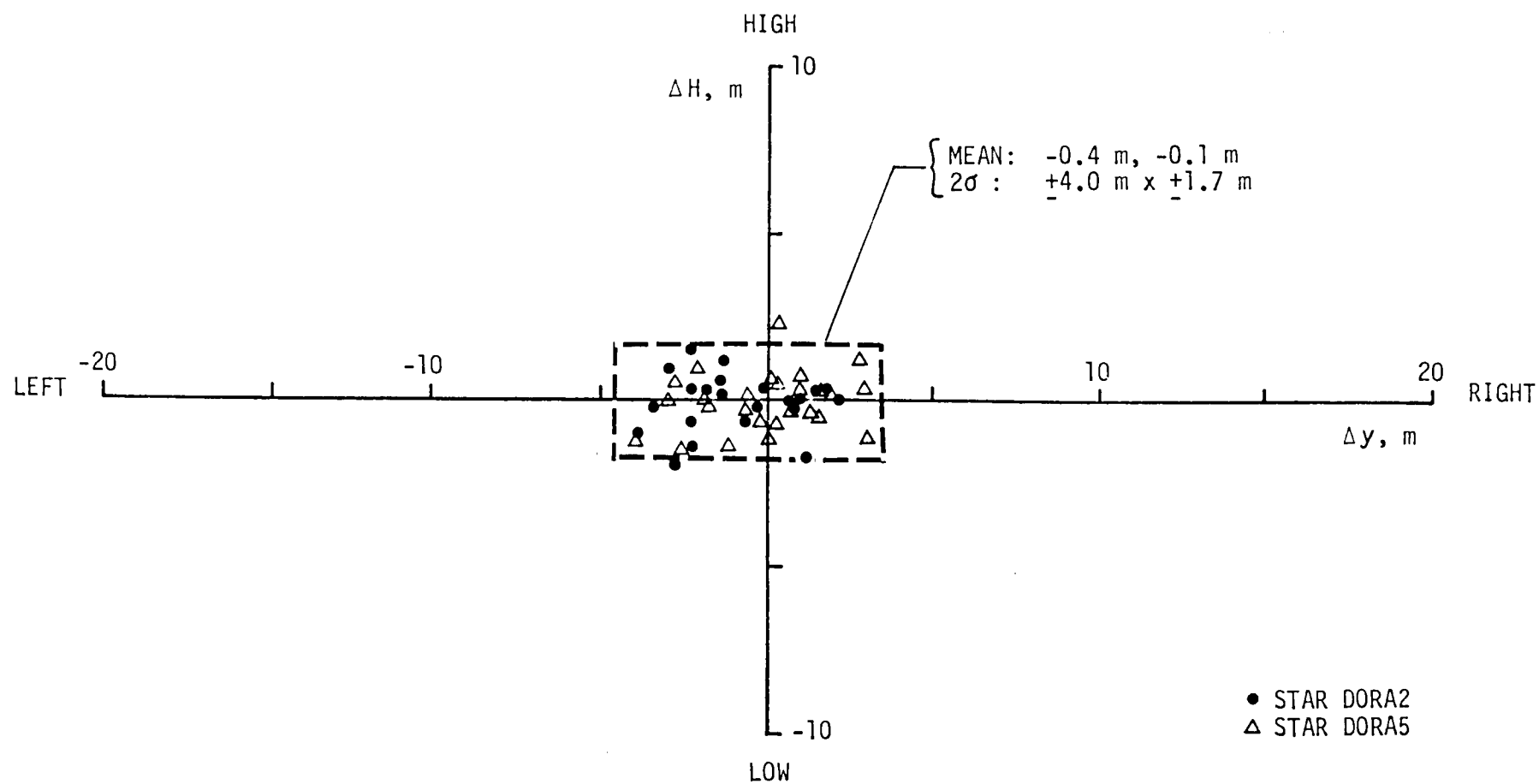


Figure 19. - Summary of TRSB - Derived Errors at Flare Initiation for Montreal/Dorval International Automatic MLS Landings.

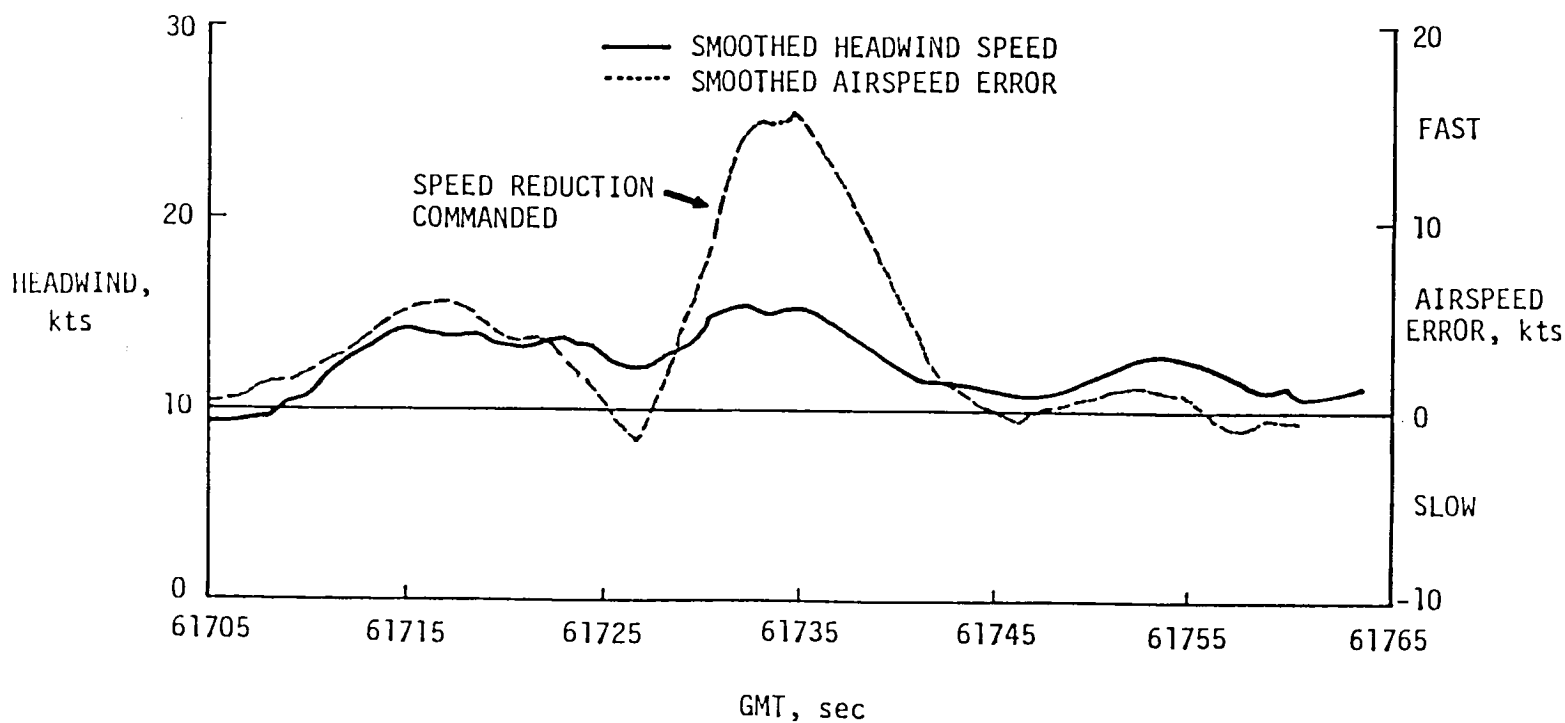
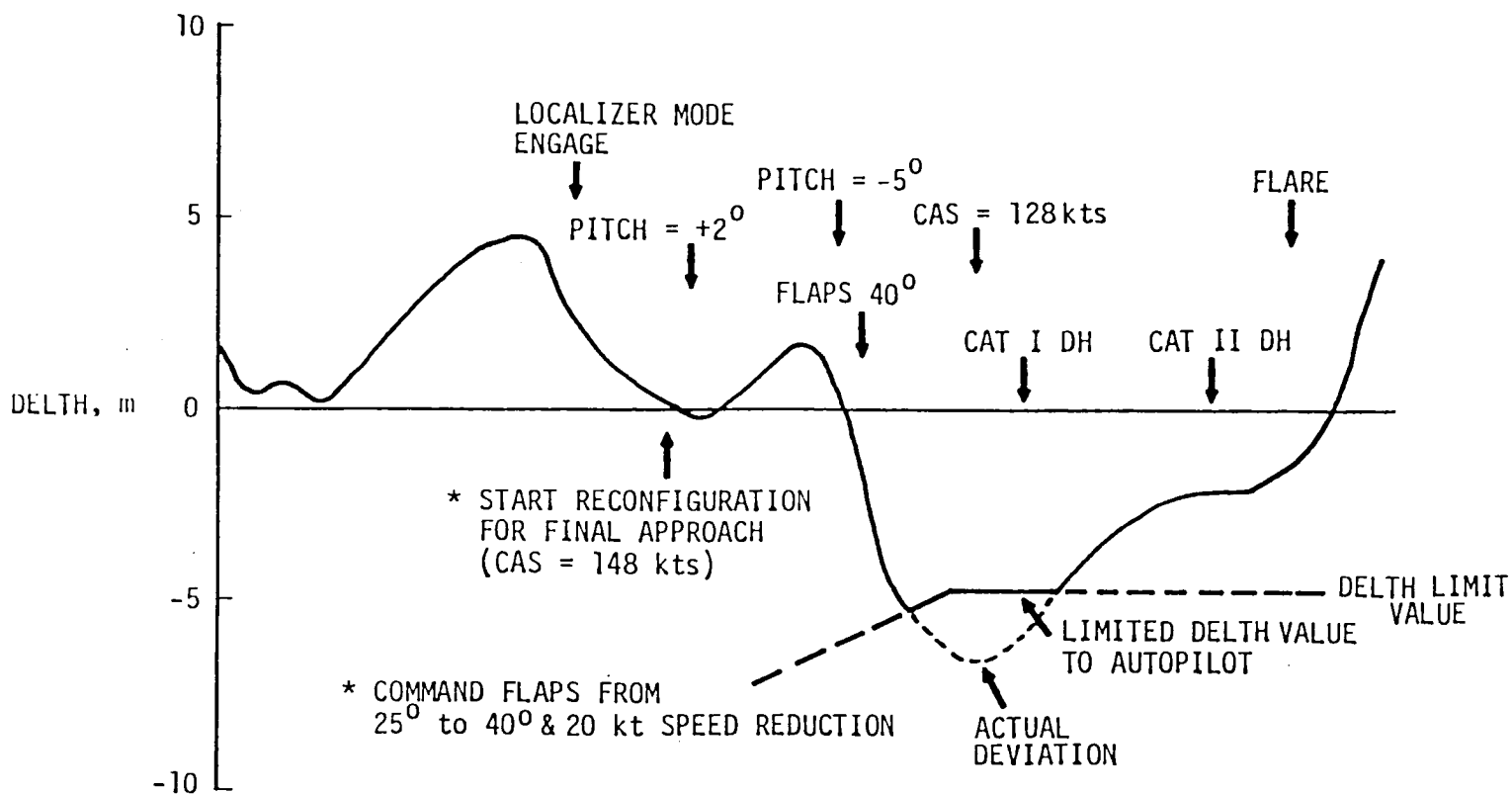


Figure 20. - Analysis of large glidepath errors on Flight/Run No. 229A-5.

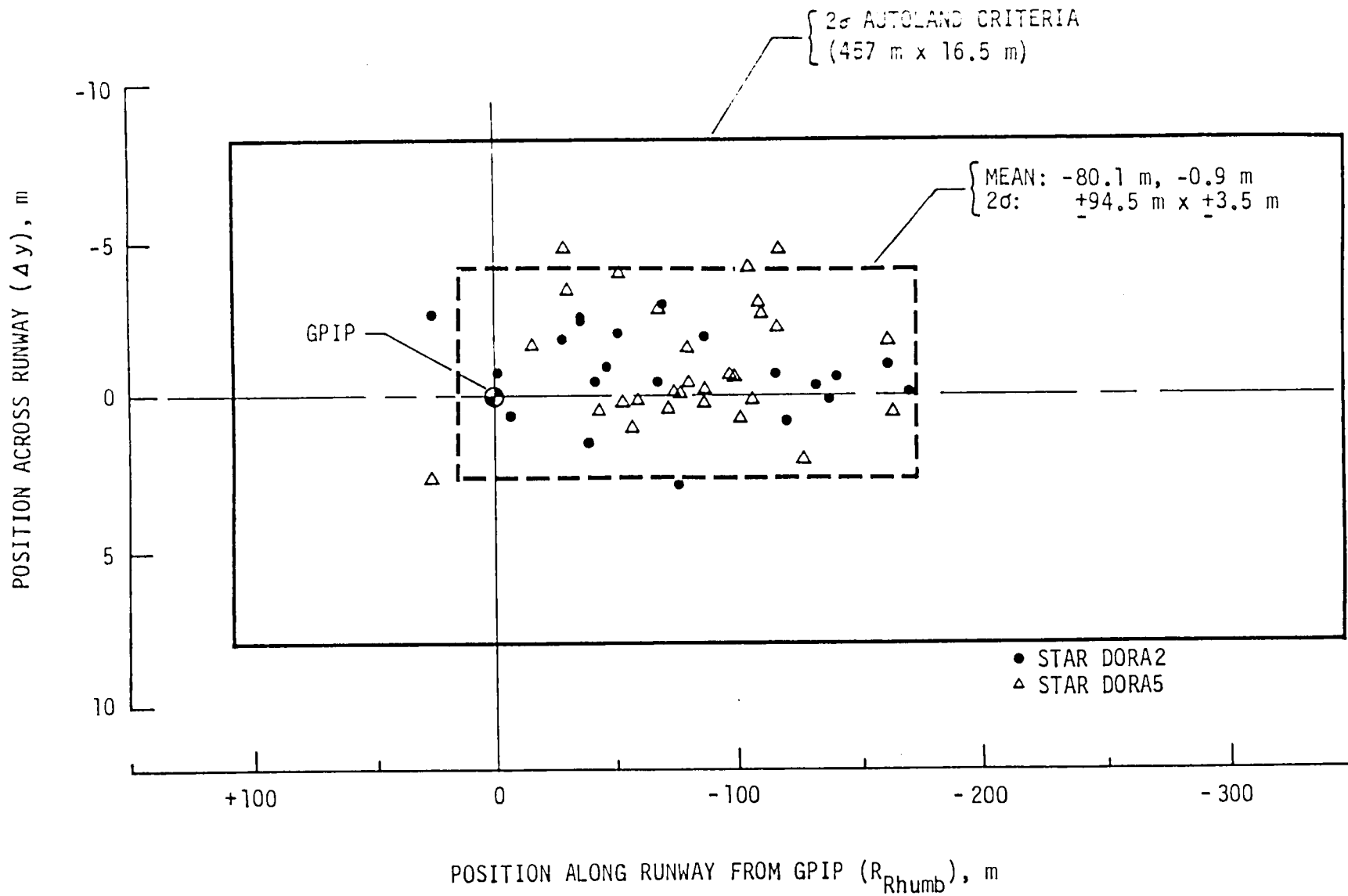


Figure 21. - Summary of TRSB - Derived Touchdown Performance of TCV B-737 for Automatic Landings at Montreal/Dorval International Airport.

1. Report No. NASA TM-81885		2. Government Accession No.		3. Recipient's Catalog No.	
4. Title and Subtitle FLIGHT PERFORMANCE OF THE TCV B-737 AIRPLANE AT MONTREAL/DORVAL INTERNATIONAL AIRPORT, MONTREAL, CANADA, USING TRSB/MLS GUIDANCE				5. Report Date SEPTEMBER 1980	
				6. Performing Organization Code	
7. Author(s) William F. White and Leonard V. Clark				8. Performing Organization Report No.	
				10. Work Unit No. 534-04-13-62	
9. Performing Organization Name and Address NASA Langley Research Center Hampton, VA 23665				11. Contract or Grant No.	
				13. Type of Report and Period Covered TECHNICAL MEMORANDUM	
12. Sponsoring Agency Name and Address National Aeronautics and Space Administration Washington, DC 20546				14. Sponsoring Agency Code	
15. Supplementary Notes					
16. Abstract The NASA Terminal Configured Vehicle B-737 was flown at Montreal/Dorval International Airport, Montreal, Canada, in support of the world-wide FAA demonstration of the Time Reference Scanning Beam/Microwave Landing System. This report presents a summary of the flight performance of the TCV airplane during demonstration automatic approaches and landings while utilizing TRSB/MLS guidance. The TRSB/MLS was shown to provide the terminal area guidance necessary for automatically flying curved, noise-abatement type approaches and landings with short finals.					
17. Key Words (Suggested by Author(s)) Microwave Landing System Time Reference Scanning Beam Landing Guidance Systems Automatic Landings Curved Approaches				18. Distribution Statement Unclassified - Unlimited Subject Category 04	
19. Security Classif. (of this report) Unclassified	20. Security Classif. (of this page) Unclassified	21. No. of Pages 34	22. Price* A03		

